AN ABSTRACT OF THE THESIS OF

Mehgan O'Hearn Blair for the degree of Master of Science in Geology presented on March 17, 2005.

Title: Sediment Storage and Delivery on Holocene Glacial Timescales, Granite Creek, Southern Alaska

Abstract Approved:

Andrew Meigs

Andrew J. Meigs

Sediment storage in and release from the Granite Creek catchment over Holocene timescales is modulated by the fluctuations of Tana Glacier, which periodically blocks the outlet of Granite Creek. Little Ice Age expansion from 1500-1900 AD is suggested by lichenometric ages of alpine glacial moraines within Granite Creek valley. Trimlines above the Tana Glacier terminus indicate that, during this period, ice was at least 120 m thicker in the Tana Valley. According to the elevation of shorelines within the valley, the resultant ice-dammed lake occupied 50 km^2 in the lower ~10 km of Granite Creek valley, contained 5.9 km^3 of water, and was at least 90 m deep at its maximum.

Removal of the ice dam occurred during twentieth century thinning of Tana Glacier and caused a 100-m drop in the base level of Granite Creek, driving evacuation of lacustrine valley fill. The reestablishment of the fluvial system was characterized by lateral migration of Granite Creek and formation of a series of paired terraces, indicating

non-catastrophic and possibly seasonal drainage of the lake. Roughly 1.3×10^8 m^3 of stored sediment has been removed from the basin since drainage of the lake. Radiocarbon ages within the valley fill reveal an unconformity between overlying sediment deposited during the Little Ice Age and underlying, older sediment dating to ~900 yrs B.P. Two episodes of impoundment and lacustrine deposition in the basin occurred during the mid-late Holocene and may have been separated by a period of incomplete evacuation of the valley fill.

These observations reveal that sediment production within, and sediment delivery out of this catchment are out of phase, which is characteristic of paraglacial landscape response following deglaciation. In southern Alaska, paraglacial landscape adjustment may explain the discrepancy between erosion rates estimated from short-term sediment yields and those from long-term exhumation rates. It is clear that the interpretation of sediment yields requires consideration of all sources of eroded sediment, including stored material, on a variety of timescales.

Sediment Storage and Delivery on Holocene Glacial Timescales, Granite Creek, Southern Alaska

by
Mehgan O'Hearn Blair

A THESIS

submitted to

Oregon State University

in partial fulfillment of
the requirements for the
degree of

Master of Science

Presented March 17, 2005
Commencement June 2005

Master of Science thesis of Mehgan O'Hearn Blair presented on March 17, 2005.

APPROVED:

Andrew Meigs

Major Professor, representing Geology

Chair of the Department of Geosciences

Sally Francis

Dean of the Graduate School

I understand that my thesis will become part of the permanent collection of Oregon State University libraries. My signature below authorizes release of my thesis to any reader upon request.

Mehgan O'Hearn Blair

Mehgan O'Hearn Blair, Author

ACKNOWLEDGEMENTS

The author gratefully acknowledges the help of Dr. Andrew Meigs, who inspired many of the ideas and interpretations put forth in this manuscript. The investigation would not have been possible without his creative and thoughtful contributions in the field. His thorough critiques and suggestions greatly improved the manuscript.

Dr. Lewis Owen generously devoted personal and laboratory time to this investigation and contributed to the author's understanding of current research in paraglacial geomorphology.

The author thanks the following people for discussions and suggestions regarding this project: Dr. Stephen Lancaster, Dr. Peter Clark, and Anders Carlson of Oregon State University, Mike Loso of the University of California-Santa Cruz and George Burr of the University of Arizona.

Sarah Johnston and Kathryn O'Hearn assisted in logistical planning and greatly improved the quality of fieldwork. Devi Sharp of the National Park Service and Kelly and Natalie Bay of Wrangell Mountain Air provided logistical support for field work in the backcountry. Financial support for this investigation was provided by Oregon State University, the National Science Foundation-Arizona Accelerator Mass Spectrometer Laboratory, and the Geological Society of America.

The author also extends thanks to those who helped her succeed at Oregon State University: Dr. John Dilles, Dr. Peter Clark, and Dr. Jay Noller offered exceptional courses/field trips which were both challenging and inspiring. Sarah Johnston, Anders Carlson, and Bob and Laika Blair offered unconditional support and encouragement.

TABLE OF CONTENTS

	Page
Introduction	1
Methods	8
Granite Creek Valley	9
Geology	9
Climate and Glacial History	10
Geomorphic and sedimentologic setting	13
Glacial geomorphology	13
Lake geomorphology	18
Morphology and sedimentology of the valley fill	21
Fluvial geomorphology	31
Numerical dating of glacial moraines and valley fill	32
Lichenometry	32
Radiocarbon	34
Discussion	37
Sequence of event in the basin	37
Volumes of sediment transfer	42
Response of unglaciated tributary catchments to deglaciation	43
Conclusions	46
References	48
Appendices	53
Appendix A Lichenometric data	54
Appendix B Volume calculations	55

LIST OF FIGURES

Figure		Page
1.	Summary of sediment production, storage, and transport in a tributary alpine catchment undergoing deglaciation	3
2.	Generalized summary of sediment transfer in glaciated landscapes and the role and modes of sediment storage	4
3.	Location of study area	6
4.	Holocene glacial chronologies for the Wrangell and St. Elias Mountains	12
5.	Geomorphic map of Granite Creek	14
6.	Tana Glacier lateral moraines	16
7.	Alpine glaciers and associated moraines along northern flank of Thompson Ridge	17
8.	Cross sections of Granite Creek Valley	20
9.	Stratigraphic sections within the valley fill and location of radiocarbon samples	22
10.	Character of lacustrine deposits in Granite Creek	25
11.	Lichenometric results	36
12.	Calibrated age ranges for radiocarbon samples	39
13.	Schematic drawing of Granite Creek Valley illustrating sedimentary packages used for volume calculations	44

LIST OF TABLES

Table Page

1. Lithofacies code descriptions..... 23

2. Lichen measurements..... 35

3. Results of radiocarbon analyses..... 38

LIST OF APPENDIX TABLES

Table Page

4. Individual lichen thalli measurements..... 54

5. Estimate of volume of material evacuated from the basin..... 56

6. Estimate of lake volume..... 56

Introduction

The Chugach/St. Elias mountain range in southern Alaska is an actively uplifting orogenic belt characterized by rapid erosion rates. In this region, however, short-term erosion rates calculated from sediment yields and long-term denudation rates measured by low-temperature thermochronometry differ by an order of magnitude (Hallet et al., 1996; O'Sullivan and Currie, 1996; Spotila et al., 2004; Johnston et al., 2004). If the temporal scale over which these rates are measured is the source of the discrepancy, a mechanism to explain increased sediment yields on short timescales is required. The observation that sediment yields to southern Alaskan fjords are a combined signal of sediment derived from primary bedrock erosion and sediment released from storage within the landscape results in uncertainty about whether those yields represent contemporary bedrock erosion, reworked sediment, or both.

One mechanism that may account for increased sediment delivery from glaciated Alaskan catchments may be an increase in the efficiency of subglacial erosion, which accompanies the rapid retreat of tidewater glaciers from their Little Ice Age (LIA) termini (Koppes and Hallet, 2002; Humphrey and Raymond, 1994). Rapid retreat and volume loss of tidewater glaciers is due to rapid calving. Ice flux to the terminus is increased as the glacier profile adjusts to shortened glacier lengths, thereby enhancing subglacial erosion. This mechanism can account for increased sediment yields, but limits the location of sediment production to one part of the glaciated landscape – the base of the glacier, and implies that sediment yields from southern Alaska fjords are, indeed, a direct measure of landscape lowering in the contributing glacial valleys.

In a glaciated landscape, however, sediment is produced from bedrock at the base of glaciers and in surrounding, non-glaciated and deglaciated regions (Figs. 1A and 2) (Evenson and Clinch, 1987; Arsenault and Meigs, in press). For example, sediment produced directly by the trunk glacier is delivered to the outwash plain via supraglacial transport, englacial transport and subglacial meltwater, where it may be stored in landforms or transported out of the basin. Sediment sourced from surrounding hillslopes is transported via mass movement to adjacent glaciers and (glacio-) fluvial networks. Sediment derived from the surrounding landscape, such as tributary valleys, may be routed through a series of catchments, stored periodically, and transported by fluvial and glacial pathways until it is delivered to the trunk glacier or outwash stream, or to offshore basins (Ballantyne 2002; Lamoureux, 1999). The sediment delivered out of glaciated basins is thus recognized as a combination of sediment produces by glaciers, rivers, and hillslopes (Fig. 2).

Sediment yields from glaciated catchments are also a compound signal of sediment eroded directly from bedrock and sediment remobilized from storage sites in the landscape (Fig. 2; Church and Slaymaker, 1989; Phillips, 1991; Hodgkins et al., 2003). Reworking and transport of stored material from recently deglaciated landscapes is an integral component of the concept of paraglacial geomorphology (Warburton, 1999; Ballantyne, 2002b), which asserts that enhanced sediment yields during deglaciation result from exposure and transport of unstable and metastable sediment sources (Church and Slaymaker, 1989; Ashmore, 1993). The paraglacial period is defined as the time over which surface processes operate to exhaust glacially conditioned sediment sources (Church and Ryder, 1972; Ballantyne, 2002a). The paraglacial response of southern

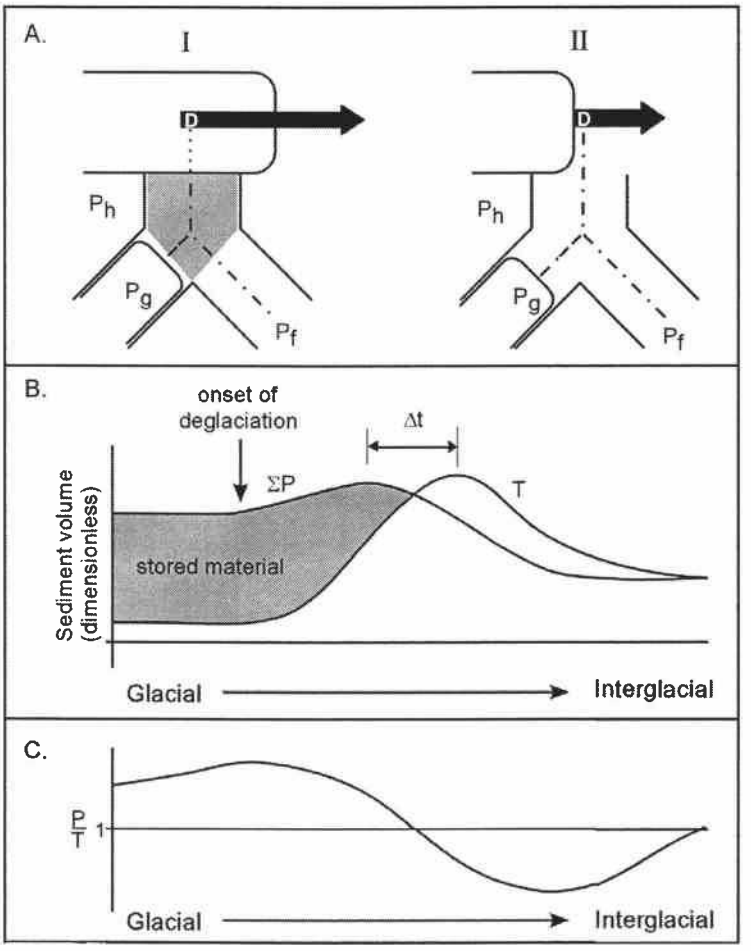

Figure 1. Summary of sediment production, storage, and transport in a tributary alpine catchment undergoing deglaciation. (A) Schematic plan of a tributary catchment during glacial maxima (I) and after glacial retraction (II). Primary sediment production in a glaciated landscape is the sum of glacial (Pg), fluvial (Pf), and hillslope (Ph) erosion. Delivery (D) out of the catchment is modulated by trunk glacier fluctuations, as it is stored behind the trunk glacier during glacial maxima (shaded). (B) The transition from glacial maxima to glacial minima is characterized by increased primary production (ΣP) from hillslopes and fluvial channels, though primary glacial erosion diminishes as glaciers thin and retreat (see text for discussion). During glacial maxima, sediment is stored in tributary valleys behind trunk glaciers; transport (T) out of the catchment is minimal. After glacial retreat, sediment stored on the landscape in the form of glacial landforms and valley fills is transported out of the basin. Δt indicates the lag time between peak sediment production and peak sediment delivery from the catchment due to storage and later release of sediment. (C) Periods of glacial advance are thus characterized by sediment storage as production (P) in upland tributary catchments is greater than transport from the basin (T). During glacial retraction, transport is greater than production, resulting in sediment release and resultant high sediment yields which do not reflect contemporary primary denudation of the landscape. Modified from Church and Ryder (1972); Hinderer (2001).

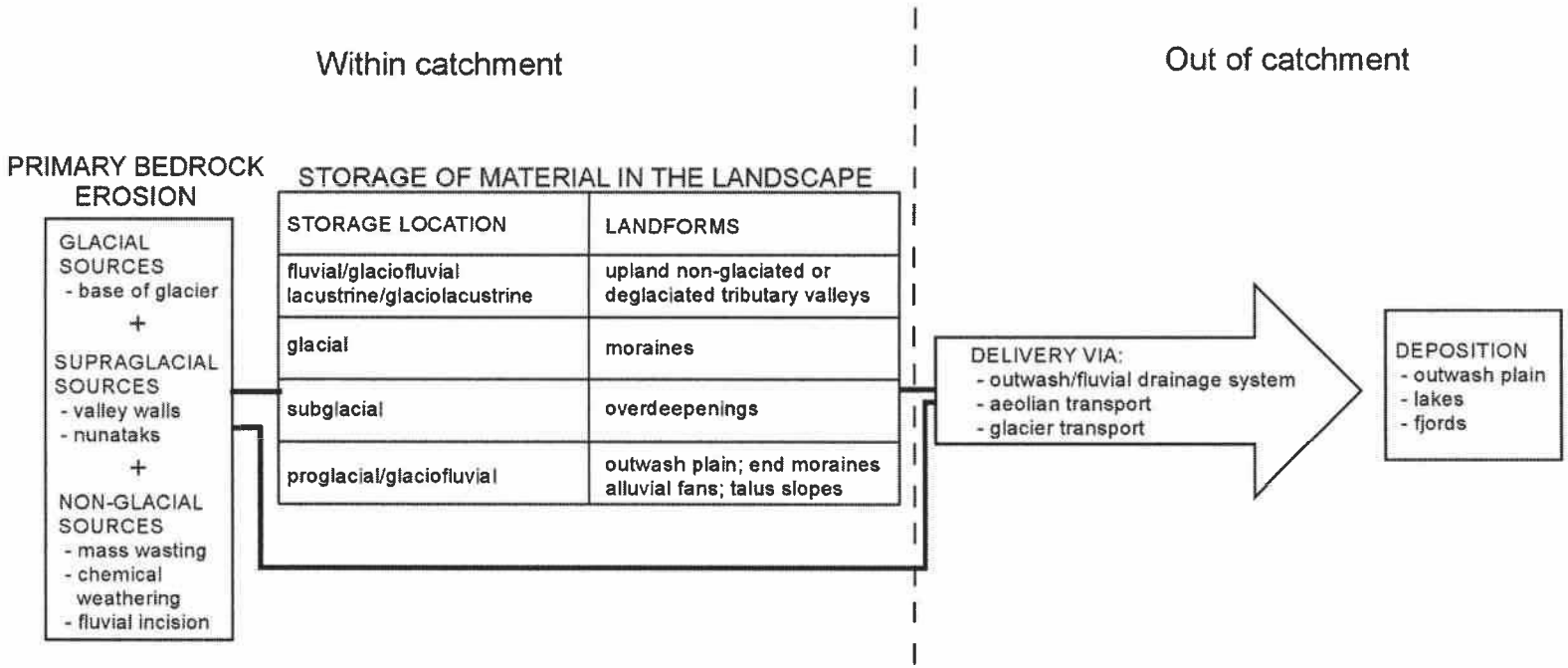

Figure 2. Generalized summary of sediment transfer in glaciated landscapes and the role and modes of sediment storage.

Alaskan landscapes to glacial retreat since the end of the Little Ice Age may provide a way to account for increased sediment yields on short time scales. In contrast to the idea that enhanced subglacial erosion is the source of enhanced sediment yields, if paraglacial adjustment on short timescales contributes to high sediment yields, it implies that these yields are an integrated signal of glacial, fluvial, and hillslope erosion, and that much of the sediment delivered out of catchments may be remobilized, so sediment yields do not reflect contemporary erosion of the land surface.

This investigation explores the role that sediment storage and release play in a landscape undergoing deglaciation. The length of the paraglacial period of landscape adjustment is controlled by 1) the availability of glacially-conditioned sediment, and 2) the rate of sediment transport. Therefore, understanding the physical mechanisms of sediment storage in and sediment release from a landscape, and the timescales over which they operate, is essential to understanding landscape adjustment to deglaciation.

In glaciated regions, trunk valley glaciers exert a primary control on sediment storage in and release from tributary valleys in glaciated landscapes. Ample space to accommodate sediment storage in unglaciated tributary valleys exists because of the linked topology of glaciated landscapes (Fig. 3). Sediment storage in and sediment release from tributary valleys over glacial cycles may be modulated by base-level fluctuations defined by the thickness or absence of glacial ice in the trunk valley. Advance and thickening of glacial ice will dam the tributary valleys and impound sediment produced in that catchment over the period of damming (Roberts et al., 2003). Retreat of the glacier past the tributary outlet will cause rapid incision of the stream and sediment release. The system may also be complicated by glacial fluctuations of various

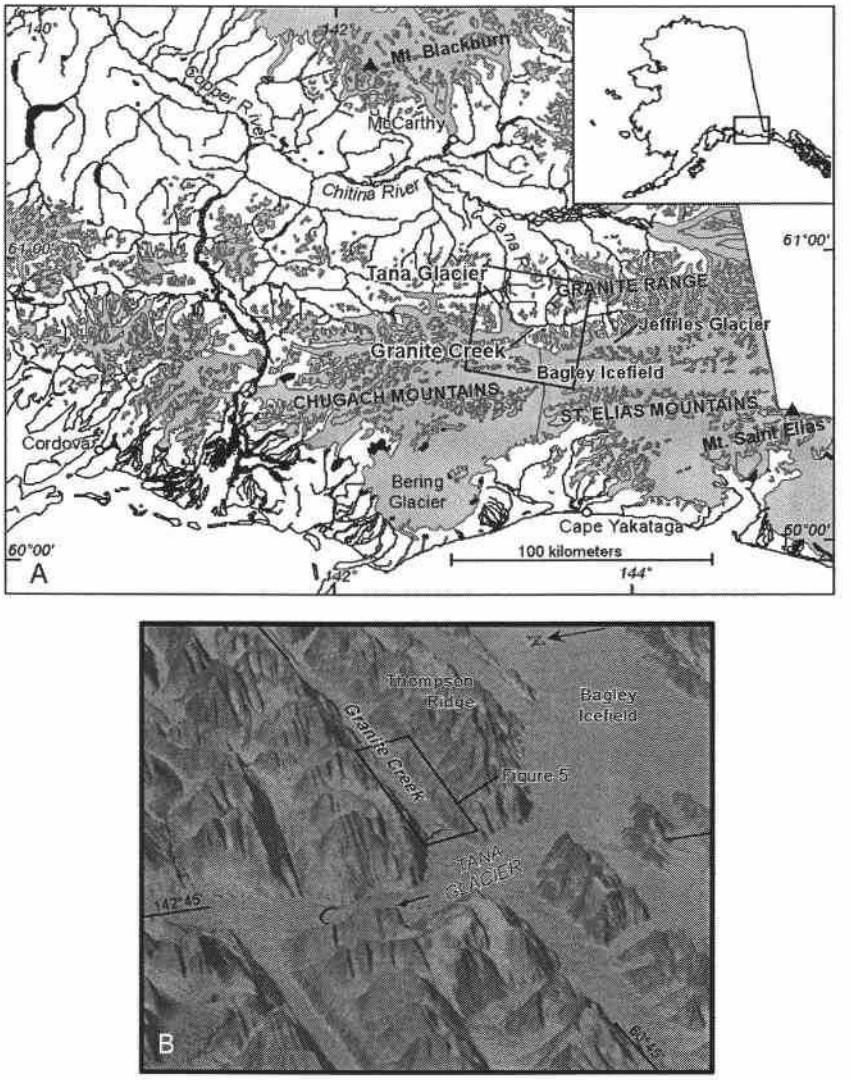

Figure 3. Location of study area. (A) Regional map of southern Alaska showing location of Tana valley, Granite Creek, and associated drainage basins. The open rectangle indicates the extent of (B). (B) View looking southeast to Granite Creek, Tana Glacier, and Thompson Ridge. Bagley Icefield feeds the north-flowing Tana Glacier. Note that base level for tributary streams oriented perpendicular to the Tana Glacier is set by the thickness of ice in the Tana Valley. Scale varies; the outlet of Granite Creek is ~2 km wide at the confluence with Tana Glacier. Data source: United States Geological Survey 30-meter digital elevation model (DEM).

timescales, causing incomplete evacuation of stored sediment. Thus, climatic changes and the concomitant changes in ice thickness of trunk glaciers potentially creates an out-of-phase relationship between sediment production in and sediment delivery out of glaciated catchments.

Figure 1 illustrates the relationship between sediment production in and delivery from a tributary catchment during deglaciation as posited by the paraglacial model. As glaciers thin, sediment production from hillslopes increases as unstable slopes become exposed. Sediment production by fluvial systems increases as they respond to base level lowering and remobilize stored sediment. Delivery out of the basin is limited during glacial maxima because colder, dryer conditions decrease the amount of meltwater, which limits the distance that sediment can be transported (Hinderer, 2001). Sediment produced in tributary catchments may be stored behind thickened trunk valley glaciers, and hillslopes are buttressed by ice in valleys. During deglaciation, increased glacial meltwater and release of tributary stores enhances sediment delivery from the basin. Storage and the delayed release of material enhance the natural lag time between the peak sediment production in and peak sediment delivery out of the catchment.

Granite Creek, a west-flowing tributary of the Tana Valley on the northern flank of the Chugach Range (Fig. 3) was formerly dammed by the Tana Glacier. Evidence for this is provided by >30 m thick valley fill, comprising rhythmically laminated mud, silt, and fine sand and by shorelines developed on alpine glacier moraines. The Tana Glacier modulates sediment delivery from this 500 km^2 catchment by impounding and storing sediment produced over a ~400-yr period leading up to the LIA maximum. In the ~100 yrs since thinning of the Tana Glacier, lacustrine sediment was removed from the lower

~8 km of the valley and the remaining valley fill is a source of suspended sediment for the reestablished fluvial system. The area thus provides an opportunity to examine the spatial and temporal link between trunk glacier fluctuations and tributary-damming, and to quantify valley filling and evacuation over Holocene-scale glacial cycles. Specifically, the objective of this investigation are as follows: 1) establish the timing of local Little Ice Age advance and retreat, 2) to establish the timing of lake impoundment and release, and 3) to estimate the amount of material removed from Granite Creek valley since removal of the ice dam.

Methods

Four data sets were developed to quantify the timing and magnitude of glacial fluctuations, sediment storage, and subsequent sediment delivery. 1) The geomorphology in the lower 8 km of the valley was mapped to determine the relative sequence of events and to reconstruct the landscape history. Terraces were mapped using a combination of mapping and collection of differential global positioning system (DGPS) data. 2) Eight vertical sections were logged to determine the depostitional environment and volume of sediment within the valley fill. Sedimentological characteristics, sedimentary structures and facies were recorded and classification of facies followed Eyles et al. (1983) and Eyles and Miall (1984). 3) The chronology of events in the basin was constrained using radiocarbon analysis and lichenometry. Seven samples from within the stratigraphic sections were analyzed for radiocarbon by accelerator mass spectrometry at the NSF-Arizona AMS Laboratory. Diameters of the thalli of crustose lichen *Rhizocarpon geographicum* were measured on sets of moraines within Granite Creek valley to

determine the timing of local glacial advances. The diameters were converted to ages based on a growth curve developed for the White River basin, located ~100 km north of Granite Creek (Denton and Karlen, 1977; supplemented by Wiles et al., 2002). 4) To calculate the volume of sediment removed from the landscape since lake drainage, the USGS 30-m digital elevation models (DEM) and the DGPS data were used to construct grids representing geomorphic surfaces within the valley. Gridding software was used to calculate volumes of the sedimentary packages.

Granite Creek Valley

Geology

Granite Creek is situated on the north flank of the Chugach/St. Elias Mountains. Bedrock exposed in Granite Creek valley consists of metasedimentary and metavolcanic rocks associated with the east-west trending Chugach Metamorphic Complex. Major structures, including the regional metamorphic foliation, also trend roughly east-west (Hudson and Plafker, 1982). Drainage patterns in the area reflect this east-west orientation, and fluvial and glacier valleys occur between elongate ridges of exposed bedrock. Granite Creek flows west towards the Tana River between Thompson Ridge and the southernmost Granite Range (Fig. 3).

The Chugach/St. Elias Range is actively uplifting due to collision of the Yakutat Terrane with the North American Plate. In this orogenic belt, erosional patterns are apparently linked to the rock flux (Meigs and Sauber, 2000) and long-term vertical denudation rates constrained by thermochronometry are ~0.4 - 3 mm yr^{-1} (Spotila et al., 2004; Johnston et al., 2004; O'Sullivan and Currie, 1996). Short-term sediment fluxes to

southern Alaskan fjords, however, suggest erosion rates of >10 mm yr^{-1}, which may be the fastest in the world (Hallet et al., 1996).

Climate and glacial history

Modern climatic conditions on the northern flank of the Chugach/St. Elais Ranges are influenced by ~ 2500-m high ridges and peaks such as Mount St. Elias and Mount Logan, which reach elevations over 5000 m. The ranges act as a physiographic barrier to weather systems coming in from the Gulf of Alaska. On the windward flank of the range, climate is modulated by incoming weather systems and the proximity of the Gulf, whereas the leeward flank of the range is characterized by extreme seasonal fluctuations of temperature and precipitation. Along the southern coast, mean annual temperature at Cordova from 1971-2000 was 5° C and mean annual precipitation was 330 cm water equivalent. Across the range on the northern flank, a station at McCarthy recorded average mean annual temperature and precipitation of -2° C and 46 cm, respectively, over the same period (Alaska Climate Research Center, 2004).

The Chugach/St. Elias Range of southern Alaska is heavily glaciated; glacial deposits that date to at least 5 Ma are found in the Yakataga Formation, demonstrating the long-term regional influence of glacial erosion (Plafker and Addicott, 1976, Lagoe et al., 1993). Glacial landforms such as overdeepened basins, extensive fjord systems, and high relief mark the southern, coastal flank of the range, whereas alpine glacial landforms such as U-shaped valleys, moraines and glacier-dammed lakes are characteristic along the northern flank of the range (Pewe, 1975; Post and Mayo, 1971).

During late Wisconsin time, the study area was covered by the northern extension of the Cordilleran Ice Sheet (Hamilton, 1994). Denton (1974) provided radiocarbon evidence for glacial maximum in the White River basin (~100 km north of Granite Creek) sometime before ~13.7 ka B.P. with almost complete deglaciation by ~ 12.5 ka B.P.

Multiple episodes of glacial advance occurred during the mid- to late Holocene in the St. Elias and Wrangell Mountains (Fig. 4; Wiles et al., 2002). In the White River basin, Denton and Karlen (1977) presented evidence for two major intervals of glacial advance, and a third, smaller advance. Four glaciers in this area experienced significant advance and moraine-building ~ 3000-2100 cal yr B.P., probably culminating ~2900-2800 cal yr B.P. based on radiocarbon and stratigraphic evidence. This glacial expansion was followed by retraction and then a short-lived glacier advance affecting 5 or 6 glaciers occurred between 1250 and 1050 cal yr B.P. No evidence was found for another glacial advance until the widely recognized Little Ice Age (LIA) advance. Two glaciers in this area are interpreted to have reached maxima by 500 cal yr B.P. (1500 AD) and LIA glacial maximum phases continued until the early 20th century.

Glaciers in the adjacent Wrangell Mountains experienced generally similar periods of expansion during the mid- to late Holocene (Wiles et al., 2002). An early advance of two glaciers ~2700-2200 cal yr B.P. agrees with an early neoglacial advance from White River. Two other glaciers experienced advance centered on ~1700 cal yr B.P. according to radiocarbon analysis of detrital organic material and overrun wood. Although Denton and Karlen (1977) did not report evidence for this advance, it may be recorded by land-terminating glaciers along the coast of southeast Alaska that

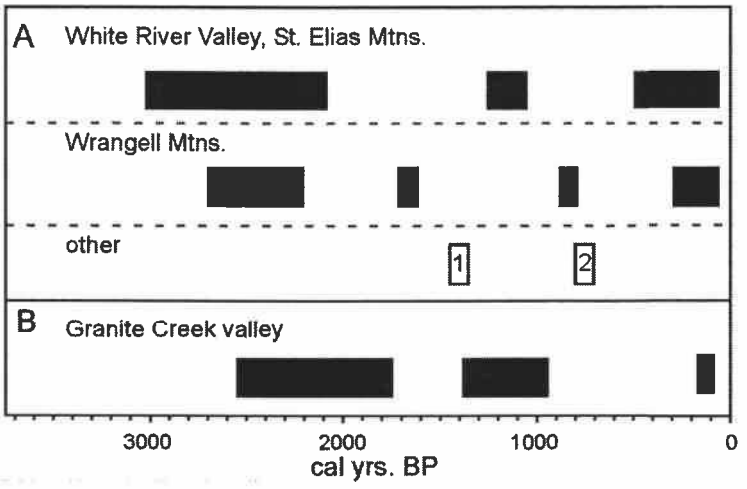

Figure 4. Holocene glacial chronologies for the Wrangell and St. Elias Mountains. (A) Summary of Late Holocene valley glacier expansion for the Wrangell (Wiles et al., 2002) and St. Elias Mountains (Denton and Karlen, 1977). Open rectangles refer to 1) advances of southeast Alaskan coastal land-terminating glaciers (Yager et al., 1998; Calkin et al., 2001) and 2) advance of glaciers in the Canadian Rockies (Luckman, 2000) and on land along the coast of southeast Alaska (Calkin et al., 2001). (B) Evidence for stabilization of moraines in Granite Creek valley based on lichenometry and radiocarbon ages presented in this work.

experienced glacial advance ~1400 cal yr B.P. (Fig. 4). Whereas White River glaciers are reported to have advanced for a short time 1250-1050 cal yr B.P., Wiles et al. (2002) argue that glaciers regionally were retracting at this time based on lack of evidence for advance by the Wrangell glaciers. Little Ice Age advances at ~800-700 cal yr B.P., ~300 cal yr B.P. (early 1700's AD), and ~100 cal yr B.P. (late 1800's - early 1900's AD) are recorded by dated moraines.

Geomorphic and sedimentologic setting

Glacial geomorphology

Tana Glacier is one of the outlets of the Bagley Icefield-Jeffries Glacier complex and occupies ~20 km in a north-trending valley (Fig. 3). Smaller alpine glaciers are supported along the length of Thompson Ridge. Granite Creek and its associated catchment lie to the east of the terminus of the Tana Valley, a tributary to the Chitina River. Preservation of end moraines downstream of the Tana Glacier is minimal. Unvegetated trimlines, however, are ~ 120 m above the present ice height near the outlet of Granite Creek.

Lateral moraines along the margins of Tana Glacier indicate at least two episodes of Holocene glacial advance and moraine-building (Fig. 5). At the confluence of Granite Creek Valley and Tana Valley, the two generations of lateral moraines stretch for 1.2 km across the outlet (Fig. 6a). The crests of the two moraines are separated by 0.5 km and both have a maximum elevation of 650 m. The eastern moraine is vegetated with alders and has a rounded morphology. The inset, western moraine is vegetated as well, though a 1978 aerial photo indicates that the western flank of the moraine was unvegetated at that

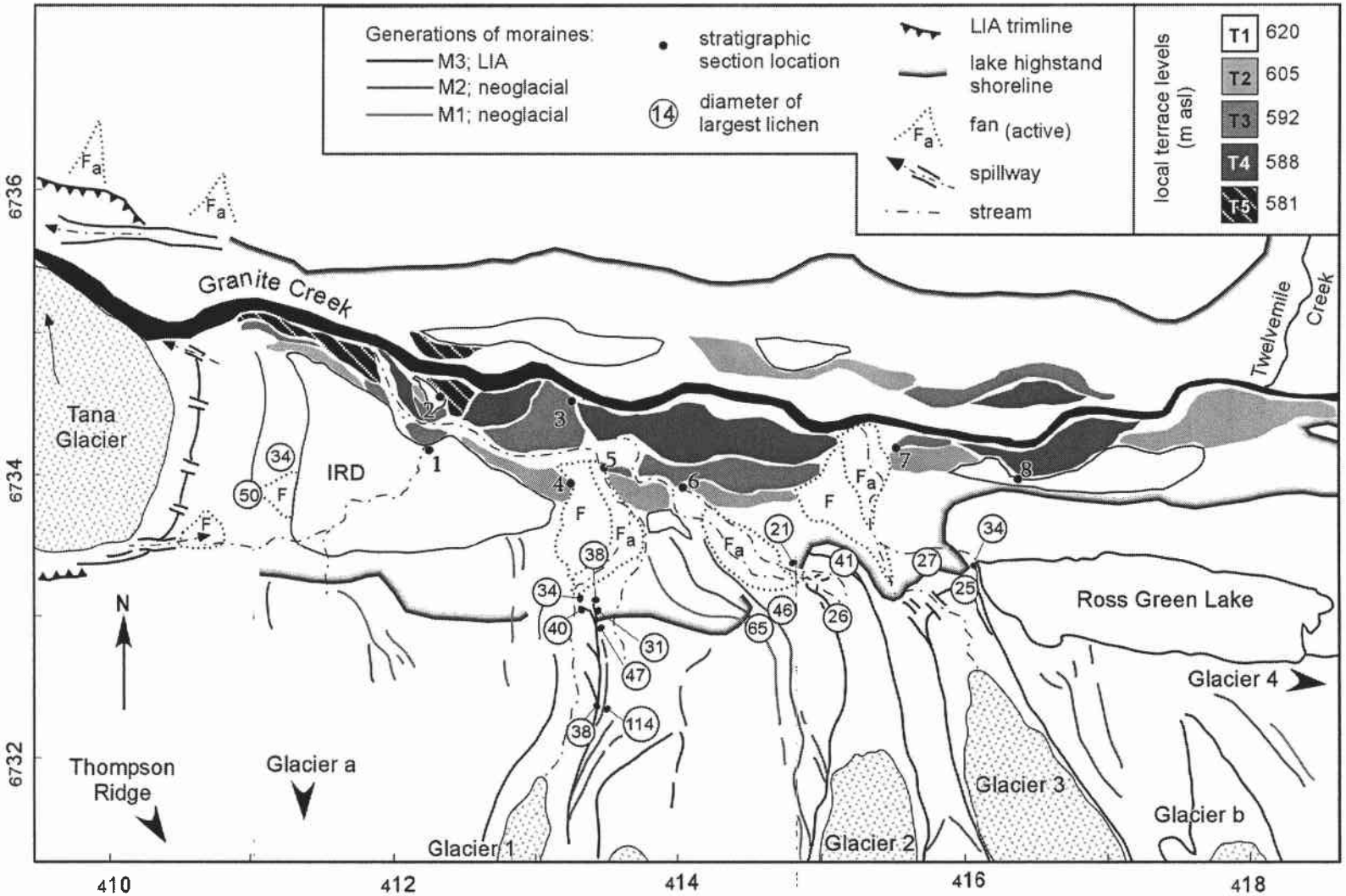

Figure 5. Geomorphic map of Granite Creek. Easting and northing in UTM kilometers. Three generations of moraines (M1-M3) were identified. Terrace level elevations (T1-T5) were measured at westernmost exposure of the individual terrace. Not all largest lichen diameters are plotted on this map.

time. The moraine is hummocky and incised along its extent.

Thompson ridge supports numerous alpine glaciers, which were lettered and numbered from west to east for mapping purposes. Moraines associated with these glaciers were mapped in the lower 8 km of Granite Creek valley (Figs. 5 and 7). Three distinct generations of moraines (M1-M3) are identified based on their relative position, extent, and morphology.

M1 moraines are furthest-removed from present glacier termini and occur outside of the M2 crests with respect to the glaciers. They have a subdued morphology and are vegetated with mats of moss and ground shrubs and dense alder (Fig. 7A). Lichen thalli are difficult to measure on these moraines, as they have grown together or the available surfaces are covered in moss and ground shrubs. M1 and M2 moraines often occur in tandem and appear as a pair of vegetated ribs trending down the slope of Thompson Ridge. Slight mounds represent the extent of these landforms onto the valley floor (Fig. 7B). M2 glacial moraines occur between M1 and M3 moraines. Lichen thalli on these moraines are large (some >100 mm in diameter) and abundant. M2 moraines are associated with all the glaciers in the mapping area. They occur on the west side of glacier 2 and the east side of glacier 3, but not between these two glaciers, indicating the two glaciers may have coalesced during that advance (Fig. 5).

The M3 moraines have steep slopes and sharp crests, and are only slightly vegetated with lichen, moss and sparse alders. All the glaciers along Thompson Ridge formed M3 moraines. Retraction of the glacier termini from the M3 position varies between 0.7 and 1.3 km.

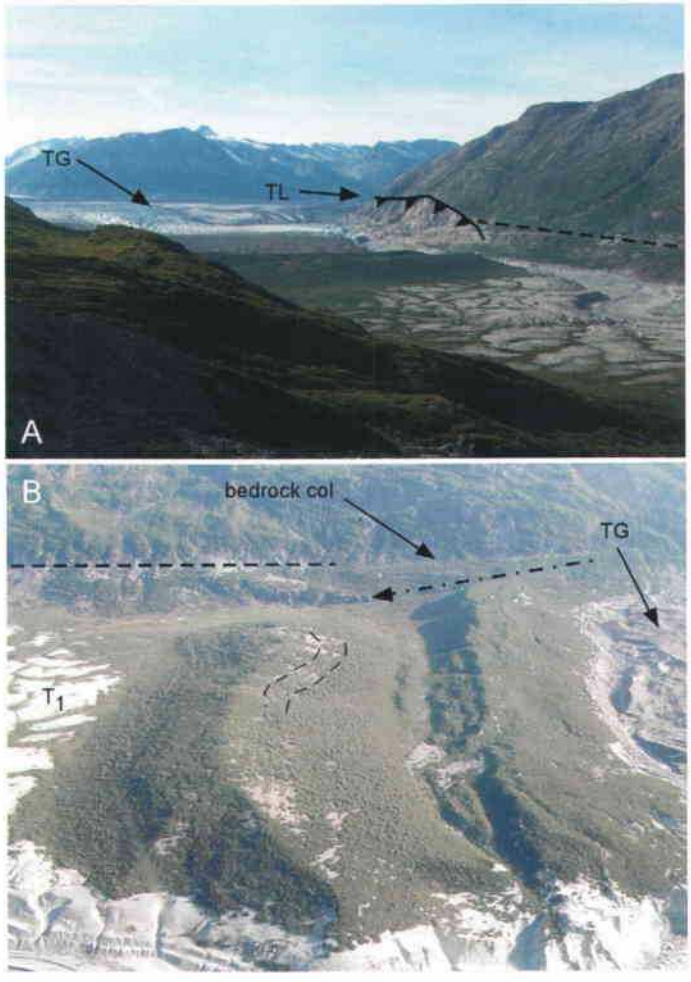

Figure 6. Tana Glacier lateral moraines. (A) View west down Granite Creek valley; Thompson Ridge is in foreground. Lateral moraines 1.2 km long block the outlet. Tana Glacier (TG) is in the background, and the LIA trimline (TL) is indicated. The dashed line represents lake level highstand. (B) View of Tana Glacier lateral moraines looking south. The dashed line represents lake level highstand. Note concentric "rings" around eastern moraine, which correspond to sorted gravel shorelines. The western moraine (on right) is dissected by spillways; the dot-dashed arrow indicates the direction of flow from an ice-marginal stream into the lake (see text).

Figure 7. Alpine glaciers and associated moraines along the northern flank of Thompson Ridge. (A) View to the southeast of Glacier 1 (G1), with associated moraines (M1-M3) extending down Thompson Ridge. Glacier b (Gb) is at a higher elevation with an M3 moraine loop. Glacier 2 (G2) can be seen in the upper left corner. (B) View to the southeast of Glaciers 2 and 3, with prominent M3 moraines; Ross Green Lake (RGL) is impounded by a Glacier 3 lateral moraine. M1 and M2 moraines indicate a coalesced advance of the two glaciers with low-profile moraines spreading onto the valley floor. Vantage point for (C) is indicated by the star. (C) Shorelines are evident as parallel lines of sorted gravel separated by roughly 1 vertical meter. (D) M3 moraine loops adjacent to Glacier 4 have a subdued morphology below 710 m elevation.

At least three episodes of glacial advance are revealed by the glacial geomorphology in the study area. The M1 and M2 moraines likely represent advances that took place during the mid-late Holocene. The M3 moraines correspond to the most recent Holocene glacial advance. At this time, the outlet of Granite Creek was blocked by Tana Glacier ice which thickened to at least 120 m above its present surface. Although Tana Glacier trimlines appear 120 m above the present glacier surface near the terminus, no coincident end moraines have been preserved in the Tana Valley. Evidently, the loss of ice volume during recent glacial retreat may have been dominated by glacier thinning and detachment of active ice from a ~7 km long swath of hummocky, debris covered, stagnant ice which characterizes the present terminus of Tana Glacier.

Lake geomorphology

Granite Creek has a catchment area of 500 km^2 and flows west toward Tana River valley. The principal tributaries include meltwater from an unnamed glacier to the east and from alpine glaciers on Thompson Ridge, and Twelvemile Creek, which originates from a small (3 km^2) icecap in the Granite Range to the north of Granite Creek.

The history of impoundment of Granite Creek is recorded in geomorphically altered landforms within the valley. A series of sorted gravel benches commonly occur between the elevations of 630 m and 710 m on M3 moraines of glaciers 1-3 (Fig. 7C). These benches also appear on the Tana Glacier lateral moraines (Fig. 6B). Moraines below these markers have subdued morphologies (Fig. 7D).

The Tana Glacier lateral moraines are incised with channels up to 5 m deep (Fig. Fig. 6B). Several of these have associated fans developed on one side of the lateral

moraine or the other. Dissected bedrock is also apparent on either side of the valley below 710 m elevation.

The legacy of lake formation, stabilization, and drainage is recorded by a diverse suite of landforms within the valley. The gravel benches associated with M3 moraines in Granite Creek valley are interpreted to be relict shorelines. The highest shorelines occur at 710 meters, which probably represents the highest stable lake level in the basin (Fig. 8A). The lake apparently covered the lower M3 moraine loops associated with glacier 4, which occur 8.5 km to the east of the outlet of Granite Creek (Fig. 7D). At its maximum, the lake also completely covered the two Tana lateral moraines at the outlet of the valley. The series of at least 30 shorelines below 710 m probably formed during lake-level drawdown and represents periods of relative stability. Incisions along the western lateral moraine (Fig. 6B, Fig. 8B) are interpreted as spillways between the lake and the Tana valley. Fans prograding into the lake basin indicate that the southern spillways were influent spillways, and a bedrock col along the southern margin of the valley may have routed water from a lateral meltwater channel along Tana Glacier into the lake basin (Fig. 8B). Another bedrock col occurs along the northern margin of the valley at an elevation of ~690 m. This channel is deeply incised and widens to the west. It likely represents an effluent spillway associated with lake level highstands (Fig. 8).

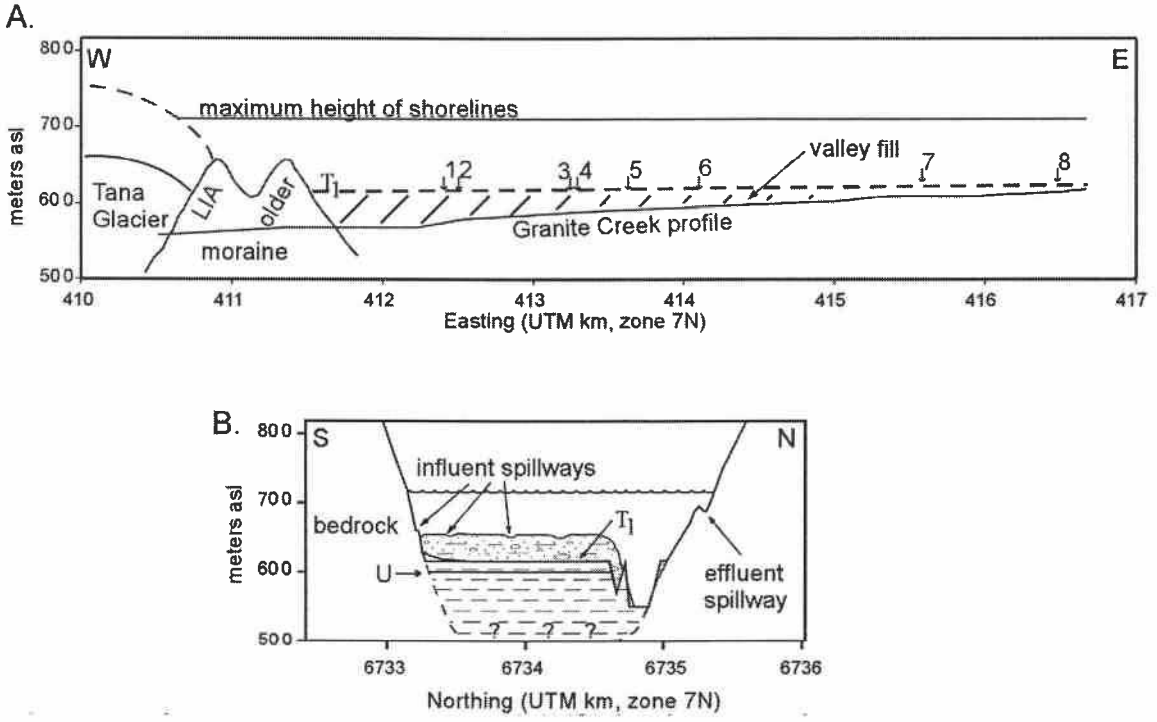

Figure 8. Cross sections of Granite Creek Valley. (A) Longitudinal profile of Granite Creek. Trimlines indicate Tana Glacier was ~120 m higher during the LIA maximum. At its maximum height, water level reached an elevation of 710 m. The T1 surface represents the highest terrace level. Granite Creek has incised through valley fill; numbers indicate locations of measured sections in Fig. 9. Presently, Granite Creek is incising through lacustrine deposits and tills of the lateral moraines of the Tana Glacier on the west. (B) Composite cross-section near the outlet of Granite Creek. An unconformity ("U") at 600 m elevation is suggested by stratigraphic and radiocarbon evidence within section 1.

Morphology and sedimentology of the valley fill

The incision of Granite Creek and formation of terraces provides a cross-sectional exposure of the valley fill (Fig. 8). A total of eight vertical sections were measured, facies were designated, and sedimentary structures noted in the field. A summary of the sedimentology for each vertical section is presented below (Fig. 9; Table 1).

Section descriptions

Section 1 was exposed by incision into T1 of an ephemeral stream that originates from a marsh in the southwest corner of the valley. The section location lies east of the Tana lateral moraines on the T1 surface, which has been protected from incision by Granite Creek (Fig. 5). Roughly 13 m of section were logged.

Laminated silts and muds dominate section 1. The thickness of beds and grain size are variable, and load structures and ripples are common. Alternating beds of fine to medium, horizontally laminated (occasionally poorly sorted) sand and laminated or deformed mud (Sh/Fl(w)) characterize most of the section (Figure 10D). A thick package of horizontally laminated silt and fine sand containing dewatering structures occurs between 3.5 and 4.5 m. This package is characterized by layers of organic-rich and oxidized horizons. Abundant grass occurs in ~few centimeter-thick mats and wood appears sporadically.

Section 2 is exposed on the northeast face of a remnant mesa of fill between the main channel of Granite Creek and a fluvial channel draining the glaciers along Thompson Ridge (Fig. 5). The exposed face rises up to 36 m, and had a freshly exposed

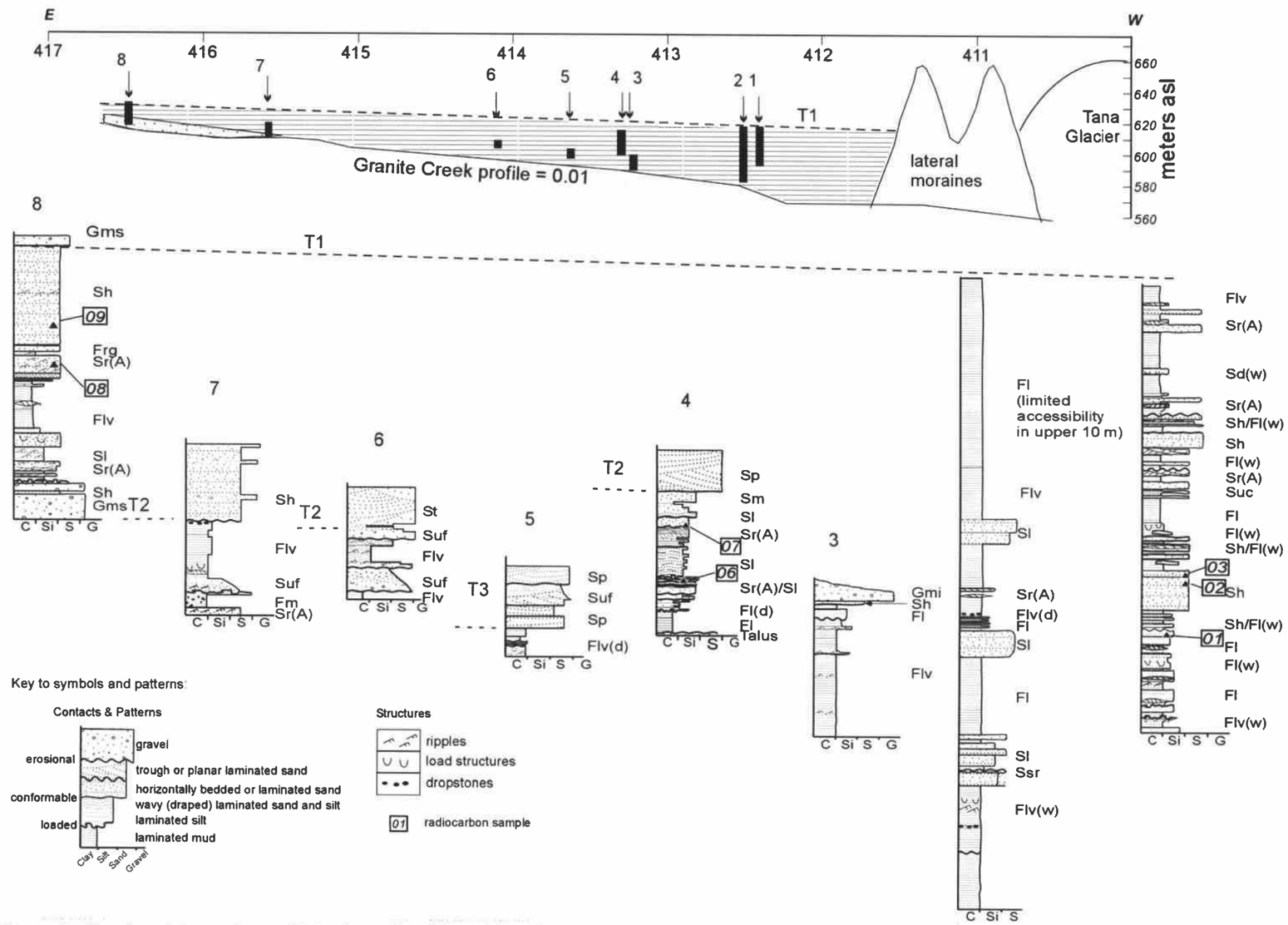

Figure 9. Stratigraphic sections within the valley fill and location of radiocarbon samples. See Fig. 5 for location of sections and table 1 for facies code descriptions. A shift in facies from east to west up Granite Creek valley indicates upstream migration of the lacustrine/fluvial interface. Fluvial sand and gravel caps occur on nearly all the sections (T1-T3) indicating erosion and deposition during incision of Granite Creek.

Table 1. Lithofacies code descriptions. Classification after Miall (1978) and Eyles et al. (1983). Abundance is reported in percent of total length logged.

	Lithofacies Codes	Description	Abundance (% Total)
Silt & Clay	Flv	Rhythmically laminated couplets of dark brown mud and lighter gray silty mud; may be capped by a 4-8 mm silt layer. Fine sand or silt stringers common. Occasional dropstones (pebble-cobble size). Occasional starved ripples 0.5-1 cm in amplitude, 5-10 cm in wavelength. Occasional evidence of dewatering or syn-sedimentary deformation (flame structures, rip-ups, intraclasts).	32.6
	Fl	As above, but may not be rythmically laminated, or many contain abundant sedimentary structures obscuring primary rhythmic deposition.	22.6
	Flm	Dark grey silty mud, with no apparent bedding. Occurance is characterized by massive and obscured bedding, contains rounded cobbles, and may be an artifact of recent slumping of section.	0.8
		Total mud:	56.0
Sand	Sl	Yellow-buff fine sand and silt, horizontally laminated (draped). May be dominated by light grey silt with dark mica ripples. Lamination is <1 mm - >1 cm thick, and assumes shape of underlying bedforms. Beds may contain various amounts of mud.	12.4
	Suf	Poorly sorted, normally graded from very-coarse sand to mud. Also occurs as a unit of upward-fining ripple drift in section 7. Occurs in packages 0.5 m-1m thick.	3.5
	Suc	Occurs in section 2 as interbeds of yellow-buff fine sand increase upwards in frequency and thickness.	0.4
	Sm	Massive sand. Same as in Sl, above, but without lamination or bedding.	0.6
	Sr(A)	Ripple cross-lamination, (A) indicates lee-side preservation, net erosion on stoss side. Occurs sporadically in sections, and is usually overlain by Sl. Ripples defined by mica concentration. Occasionally deformed.	1.4
	Ssr	Single set of type A cross-laminated rippled sand, as in Sr(A) above. No climb apparent, indicates migration without net deposition.	minor
	Sh	Horizontally bedded/low-angle cross laminated very fine to coarse sand.	16.3
	Sp	Planar cross-beds in medium to coarse sand.	4.1
	St	Trough cross-beds in medium to coarse sand.	2.0
	Se	Crudely cross-bedded or scoured medium to very coarsd sand.	minor
	Sd	Deformed sand horizons. Bedding obscured.	minor
		Total sand:	22.4
Gravel	Gmi	Massive imbricated pebble-cobble gravels	1.2
	Gms	Massive matrix-supported pebble-cobble gravels.	2.2
		Total gravel:	3.4
	___(w)	With dewatering structures	
	___(d)	With dropstones.	

face in August 2003. One year later, Granite Creek eroded the mesa, and the face retreated southward ~80 m, until only a small portion of the mesa remained. By August, 2004, water had abandoned the surface below the face, and debris accumulated at the bottom of the face.

The lower 12 meters of section 2 are dominated by rhythmically laminated muds and silts (Flv; Figs. 9 and 10A). These rhythmites vary in thickness from a few millimeter's to ~ 2 cm, and are characterized by a thick dark brown horizon overlain by a thinner, finer-grained, light gray layer. Interbedded fine sand stringers <1 mm – 2 mm thick are common. Very thin (1 mm), poorly sorted, coarse sand to pebble layers interpreted as dropstone horizons are less common, but occur several times in the section. Thin starved ripples (Ssr) occur occasionally in the section, as do deformed horizons containing flame structures, loads casts, and other indicators of dewatering and soft-sediment deformation (Figure 10B, D). Several places in the section, thicker (~1 m), fine-medium sand packages occur. These packages are horizontally bedded (Sh), and occasionally contain single sets of starved ripples, or a few cm thick layer of climbing ripples (Scr) indicating westward flow.

Section 3 is also made up almost entirely of laminated mud and silt (Fig. 10A). Five meters were logged from a freshly exposed section very close to the active channel of Granite Creek, where recent incision is evidenced by bank failure (Fig. 5, Fig. 10G). Several sharp contacts and packages of coarser material occur in the upper ~1 m. The section is capped by ~0.5 m of pebble-cobble gravel above a sharp erosive contact.

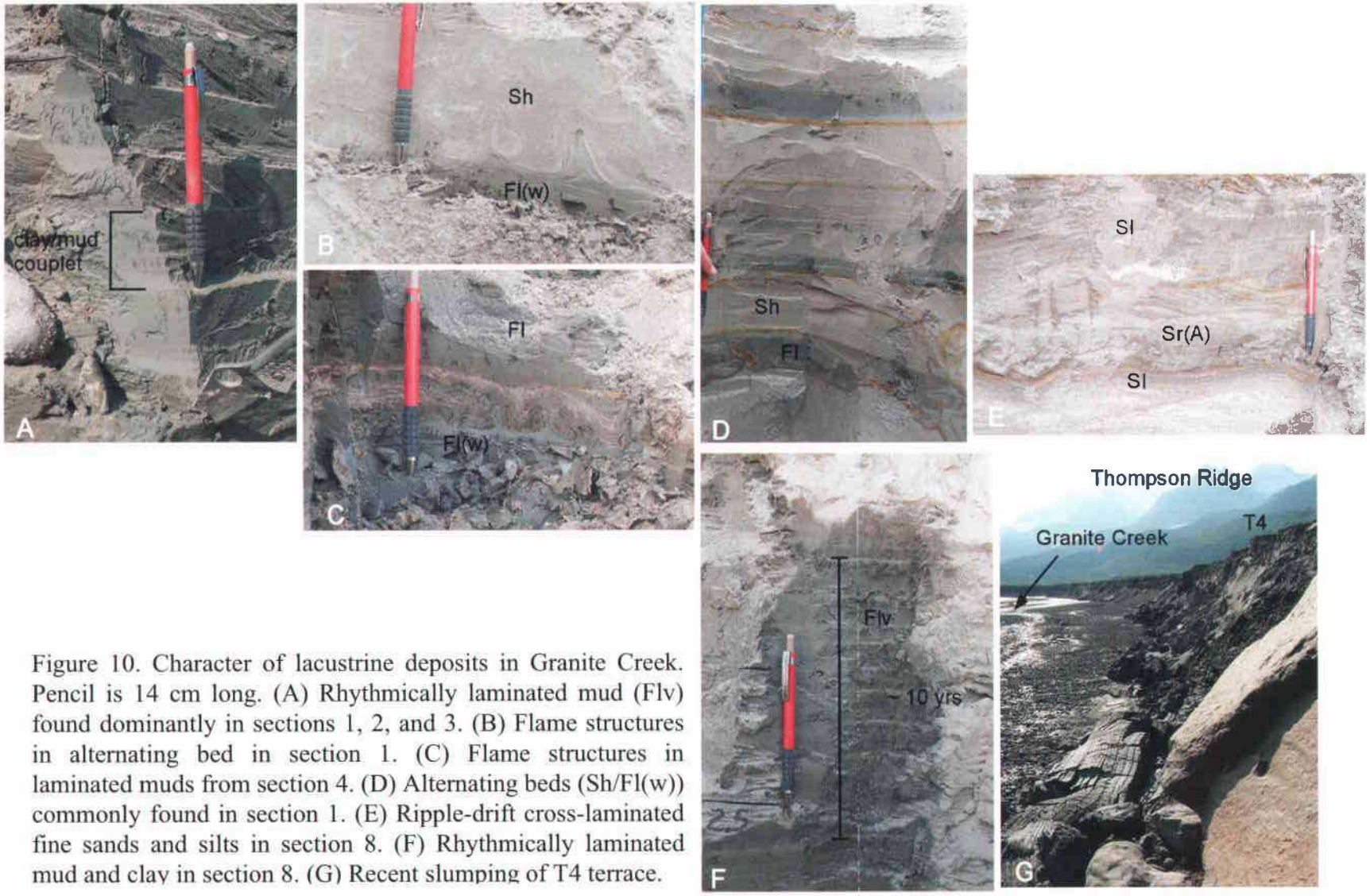

Figure 10. Character of lacustrine deposits in Granite Creek. Pencil is 14 cm long. (A) Rhythmically laminated mud (Flv) found dominantly in sections 1, 2, and 3. (B) Flame structures in alternating bed in section 1. (C) Flame structures in laminated muds from section 4. (D) Alternating beds (Sh/Fl(w)) commonly found in section 1. (E) Ripple-drift cross-laminated fine sands and silts in section 8. (F) Rhythmically laminated mud and clay in section 8. (G) Recent slumping of T4 terrace.

Section 4 was exposed by trenching into the side of a T2 surface (Fig. 5). An erosional contact at 3.8 m separates fine-grained laminated and ripple-drift cross-bedded sediments from overlying planar cross-bedded and scoured fluvial gravels. The section is dominated by laminated silt and fine sand and contains dewatering structures at 0.7 m where silt and fine sand overlie muds of the lower section (Fig. 10C). Convolute lamination and deformed ripples dominate a section of interbedded muds, silty muds, and silts from 0.7 - 1.5 m. Wavy laminated silt with interbedded horizons of increased clay content overlies this section, and is similar to the alternating beds seen in section 1, although grain size is not as variable. Draped lamination and ripple-drift cross-laminated silts and fine sands occur at 2.5 - 3.5 m, and are overlain by massive fine sand 0.3 m thick.

Section 5 was exposed by recent slumping due to incision of a meltwater stream into terrace levels T2 and T3 (Fig. 5). An erosional bounding discontinuity occurs between finely laminated and deformed muddy silt and overlying planar cross-bedded fluvial sand and gravel (Sp).

Section 6 is a ~5 m section exposed by the meltwater stream from glacier 2 (Fig. 5). The fresh exposure reveals three distinct fining-upward packages 0.5 m to 1.2 m thick separated by wavy erosional discontinuities. These packages range from poorly sorted pebble gravels to laminated muddy silt, and dramatic, but conformable, changes in grain size are the norm. A thickness of laminated rhythmites in the middle of the section contains crude ripples indicating an eastward flow regime at 1.3 m; 20 cm above, climbing ripples indicate a westward flow regime and an overall increase in grain size.

Section 7 was excavated along a south-facing side of a T2 terrace (Fig. 5); 4.5 meters of vertical section were logged. The base of the section consists of rippled fine-medium sands (Sr(A); Fig.10E), overlain by a sharp, oxidized boundary and a ~0.5 m thick unit of dark grey silty mud containing rounded cobbles (<10%). Overlying this mud is a very thin layer of pebble and cobble gravel; a layer of upward-fining ripple-drift cross-laminated sand is draped on this horizon. The boundary between the upward-fining sands and overlying laminated muds and silts is gradational and characterized by ripple-drift cross lamination. Varying amounts of mud in these laminated fines result in a rhythmic "striped" pattern of clean and dirty silt. An abrupt, erosional break between laminated muds and overlying horizontally laminated medium sand with occasional thin (~0.1 m) pebbly horizons occurs at 2.6 m. The top of T2 has been deflated, leaving a pebble lag.

Section 8 is the easternmost vertical log, and was exposed by excavation of the upper parts of a T1 terrace (Fig. 5). The lower part of the section was covered by talus. Matrix-supported gravel is immediately overlain by horizontally laminated and ripple-drift cross-laminated fine sand (Fig. 10E), which dominated the section. A roughly 1.5 m thick unit from 2.5 – 4.0 m is characterized by rhythmically laminated clay and mud (Fig. 10F). The mud layers are ~1.0 cm thick and the clay layers are ~0.5 cm thick, with a sharp contact between the clay and overlying mud. This unit is overlain by ripple-drift cross-lamination with climbing ripples indicating westward flow. A thin 0.5 cm – 1 cm mud layer separates an overlying unit of well sorted, thinly bedded (3-5 cm), buff to white fine sand. This unit is nearly three meters thick and is capped by moderately sorted

medium-coarse sand with occasional pebbles and fine sand stringers. The top of the terrace is deflated.

Interpretation of sedimentology

Evidence for lake filling, stabilization, and draining is revealed by sedimentological interpretation of facies exposed in the valley fill (Fig. 9). Sections 2, 3, 7, and 8 lie along a centerline of the valley (Fig. 4) from west to east, and are the least likely of all the sections to be influenced by input from tributary meltwater streams and adjacent hillslopes. Thus, these sections may generally represent facies deposited during eastward valley flooding and westward emptying. Sections proximal to meltwater streams may reveal complicated interfingering relationships between valley-filling and tributary stream sediment input.

Taken together, the shift of facies recorded in these sections from rhythmically laminated muds and silts in the west to ripple-drift cross-laminated fine sands and gravels in the east is interpreted to represent the eastward migration of the lake/river interface (Fig. 9). Where section 2 records 10's of meters of rhythmites, only 1.2 m of clay/mud couplets are revealed in section 8. Occasional starved ripples and ripple-drift cross-lamination occurrences in the rhythmites of sections 2 and 3 are interpreted to be distal equivalents of the dominant rippled and laminated sediments in sections 7 and 8. These facies record upstream shifts of glaciolacustrine deltaic deposition into a lake (Gustavson et al., 1975). Though evidence for deltaic deposits (contacts between foreset and bottomset beds, dipping foresets, etc.) were not observed, a gradual shift in facies from

distal subaqueous deposition close to the ice dam to proximal fluvial deposition up valley supports a deltaic model for deposition into a lake with increasing water level over time.

Section 8 contains evidence of lake level rise, sedimentation in a lacustrine environment, lake level fall, and the reestablishment of fluvial deposition. Gustavson et al. (1975) remark that, in glaciolacustrine deltas composed mostly of sand, topset beds commonly dip less than 15° and consist mostly of ripple-drift cross-lamination. In the case of section 8, a unit of lacustrine rhythmites (Fig. 10F) is bound on top and bottom by ripple-drift cross-lamination (Fig. 10E). This facies arrangement may represent deltaic deposition prior to and following a period when the lake level was higher than this location. Section 7 may have a cyclic pattern of facies similar to this as well.

Sections 1, 4, 5 and 6 are exposed in terraces located closer to tributaries sourced from the south and record a more complicated depositional environment. A large portion of section 1, for example, is characterized by alternating beds (Fig. 10D; described above). Shaw (1977) discussed possible depositional environments for alternating beds in glaciolacustrine environments, interpreting them as either 1) proximal varves from turbidity currents on a pro-delta lakebed, or 2) accumulations on levee and interdistributary-bay surfaces by vertical accretion of overbank flows. In section 1, the alternating beds may be a product of the proximity of the section to influx of sediment from a meltwater channel that flowed along the margin of Tana Glacier and into the lake from the west (Fig. 5). This meltwater stream would contribute coarse sediment during the summer melt season, but would be shut off during the winter, resulting in alternating sets of coarse laminated sands and dewatered winter clay layers. Support for this argument comes from climbing ripples within the section that record a generally eastward

flow regime. This evidence would favor a tubidity current originating from the west. Alternatively, the alternating beds may indicate back-filling of Granite Creek's channel during initial lake-filling, and subsequent overbank deposition onto the adjacent surface, which was preserved at a higher elevation behind the Tana Glacier lateral moraines. In this case, the source for the coarse layers is the main influent channel, Granite Creek, followed by shut-off of the source and settling of fines during the winter. This interpretation seems reasonable due to the proximity of section 1 to the main channel of Granite Creek.

Sections 4 and 5 are both located near the meltwater stream from glacier 1. Both sections consist of highly deformed laminated mud and silt overlain by more than 1 m of planar laminated gravels. The lower parts of these sections indicate a lacustrine environment, where deformation is a result of subaqueous slumping on a slope. Here the slope may be a direct result of the sections' proximity to a tributary sediment source to the south. The deformed and rippled units in these sections are in contrast to the undisturbed rhythmites of section 3 to the north.

The individual Suf units with abrupt changes in grain size comprising section 6 resemble bar and channel sequences proposed by Boothroyd and Ashley (1975), where poorly sorted gravels are overlain by ripple-drift cross-laminated fines. Based on similarities to their studies on braided outwash fans, and the location of this section within glacier 2's outwash fan, these deposits likely represent post-lake-drainage deposition of mid-fan channel and overbank facies.

The sedimentology of the valley fill records backfilling of the basin during impoundment, followed by reestablishment of the fluvial system accompanying lake

drainage. A shift in facies from laminated muds to coarser ripple-drift cross-laminated sands indicates an upstream transition from lacustrine facies to glaciolacustrine deltaic facies. Section 8 may record as many as four distinct depositional environments: 1) the fluvial/glaciolacustrine deltaic environment followed by 2) elevation of the lake level and associated lacustrine deposition, 3) lake level drop and resumed deposition in a proximal glaciolacustrine deltaic environment, and 4) establishment of fluvial channel characterized by deposition of pebble-cobble gravels. Post-lake-drainage and establishment of the present fluvial system is dominated by incision of the channel into erodible fine-grained sediment and deposition of fluvial gravels, resulting in ~5 levels of paired terraces with variable thicknesses of gravel.

Fluvial geomorphology

Fill-cut terraces dominate the lower reaches of the Granite Creek valley. Many of the terraces surveyed on the south side of Granite Creek have a terrace at equivalent elevation on the north side of the river. These terraces record the progressive incision of Granite Creek following drainage of the lake. Five distinct terrace levels (T1-T5; Fig. 5) were identified, mapped and surveyed.

The T1 terrace has a maximum elevation of 620 m and is the most extensive terrace in the valley. In the lower ~1.5 km of the valley, the T1 surface is characterized by ubiquitous cobbles and boulders of various sizes and sinkholes associated with incision by small, ephemeral streams. The elevation of the T1 surface is inferred to represent the bottom of the lake. The boulder debris present in the lower valley is interpreted to be ice-rafted debris from a time when lake level stood at or above the T1

surface. Upstream, ice-rafted debris does not cap the T1 surface (Fig. 5); it is instead capped by fluvial gravels.

Terraces T2-T5 record lateral migration of Granite Creek accompanying incision through the valley fill (Fig. 5). T2 has a north-south extent of >1 km, and the lower terraces also extend across much of the valley floor. They are all capped by fluvial sand and gravel of variable thicknesses (usually 0.5 – 2m), which overlie an erosional surface developed on valley fill deposits.

Numerical dating of glacial moraines and valley fill

Lichenometry

The calibrated *Rhizocarpon geographicum* growth curve for the White River Valley (Denton and Karlen, 1977) was used to provide minimum ages of the three generations of moraines in Granite Creek Valley and of the exposure of portions of the landscape following lowering of the lake level. Note that because differentiation of various subgenera of *Rhizocarpon geographicum* is often difficult, the growth curve is considered an aggregate *R. geographicum* sensu lato (s.l.) curve. The growth curve is controlled by 10 tree-ring ages, one historical date, and two radiocarbon dates, and captures the early, "great growth", and the linear, old growth of lichen thalli (see discussion in Solomina and Calkin, 2003 p. 138). The curve was modified and used by Solomina and Calkin (2003), who recalibrated the original radiocarbon ages.

The longest axes of *R. geographicum* (s.l.) thalli on boulders on moraine surfaces associated with glaciers 1, 2, 3, 4, and b were measured (± 0.5 mm; appendix A conatins all lichenometric data). Surfaces having a low slope and moss growing between boulders

were identified as stable geomorphic surfaces appropriate for lichen measurement. Also, surfaces containing numerous thalli and not covered by other vegetation were considered viable. The largest ~30 individual thalli were recorded and the five largest were averaged in an attempt to correct for inherited lichen growth. These averages are reported on the geomorphic map (Fig. 4), and are binned in 10-mm increments in figure 11A according to their geomorphic context.

Lichen diameters measured on M1-M3 surfaces support the geomorphic evidence for three general periods of moraine stabilization during the late Holocene (Table 2). The surface containing the largest average lichen diameters was an M1 surface near glacier 4 (Figs. 7D and 11A). Intermediate average large lichen diameters were measured on M2 moraines, ranging from 38.1-105.2 mm. Note that for M1 and M2 moraines, average large lichen diameters can be quite disparate, likely owing to the paucity of individual, measurable lichen thalli in those surfaces. Composite thalli and excessive vegetation limited the usefulness of M1 and M2 moraines for lichenometric dating. However, using the averages obtained from several surfaces and combining those measurements based on their geomorphologic context, ages have been assigned to M1 and M2 moraines. Because the accuracy of lichenometry using traditional methods is thought to be on the order of ± 15-20% (Solomina and Calkin, 2003 and references therein), an error estimate of ± 20% has been assigned to these ages. Plotting the average of the largest lichen averages on the growth curve indicates that M1 moraine-building ceased by 2150 ± 430 B.P. and that M2 moraines were built by 1150 ± 230 B.P. These ages correspond well to lichenometric ages from moraines in the White River Valley (Fig. 4).

Abundant individual thalli and exposed surfaces made M3 moraines excellent candidates for lichenometric dating. Lichen thalli were also measured on surfaces below 710 m elevation that were likely covered by water during the lake-level highstand. The average largest lichen diameters ranged from 16.9-45 mm for M3 moraines, and from 17.4-40 mm for surfaces below 710 m elevation. The averages of these values correspond to lichenometric ages of 120 ± 20 B.P. and 110 ± 20 B.P., respectively. Evidently, M3 moraine surfaces became stable before this time; shortly thereafter, surfaces once covered by the lake were subaerially exposed. These data are in agreement with records describing regional glacial retreat since the end of the well-documented Little Ice Age (Porter, 1989; Calkin et al., 2001).

Radiocarbon

Suitable woody debris and grass horizons for ^{14}C dating were collected from within the valley fill (Fig. 9). These samples were analyzed for radiocarbon as the NSF-Arizona AMS facility, and the results of these analyses are presented in Table 3 and figure 12. Five samples have ages younger than 500 cal yrs B.P. Four of those five samples yielded ages that were poorly constrained between ~500-100 yrs. B.P. because fluctuations in atmospheric ^{14}C do not allow assignment of a unique age range. One sample, (sample 3, Fig. 9 and table 3) gave an age of 430 ± 90 cal yrs B.P. Collectively, these data suggest that sediments above 605 m elevation were deposited during the period 500 – 100 cal yrs B.P., supporting the inference that sediment was accumulating in the valley at the time of LIA glacial advance.

Table 2. Lichen measurements.

Substrate	Sampling identifier	No. of thalli measured	Largest individual	Average of 5 largest individuals	Average for substrate
M1 moraines	L16	8	65.4	69	107
	g	21	150.0	144	
M2 moraines	L15	17	45.5	38	76
	L9	15	114.0	83	
	f	23	120.0	105	
M3 moraines	L14	21	26.2	23	31
	L17	13	19.8	17	
	L1	46	41.0	35	
	L5	29	33.0	33	
	L7	44	47.0	45	
	L8	46	38.0	37	
	L11	34	34.0	34	
	L12	38	25.0	24	
	e	15	35.0	32	
	c	31	32.0	32	
Surfaces below 710 m elevation	L2a	55	34.0	33	27
	L2b	33	50.0	40	
	L3	21	27.0	28	
	L4	36	34.0	29	
	L6	34	31.0	30	
	L10	40	27.0	23	
	L13	17	21.0	17	
	b	8	29.0	23	
	a	11	23.0	20	

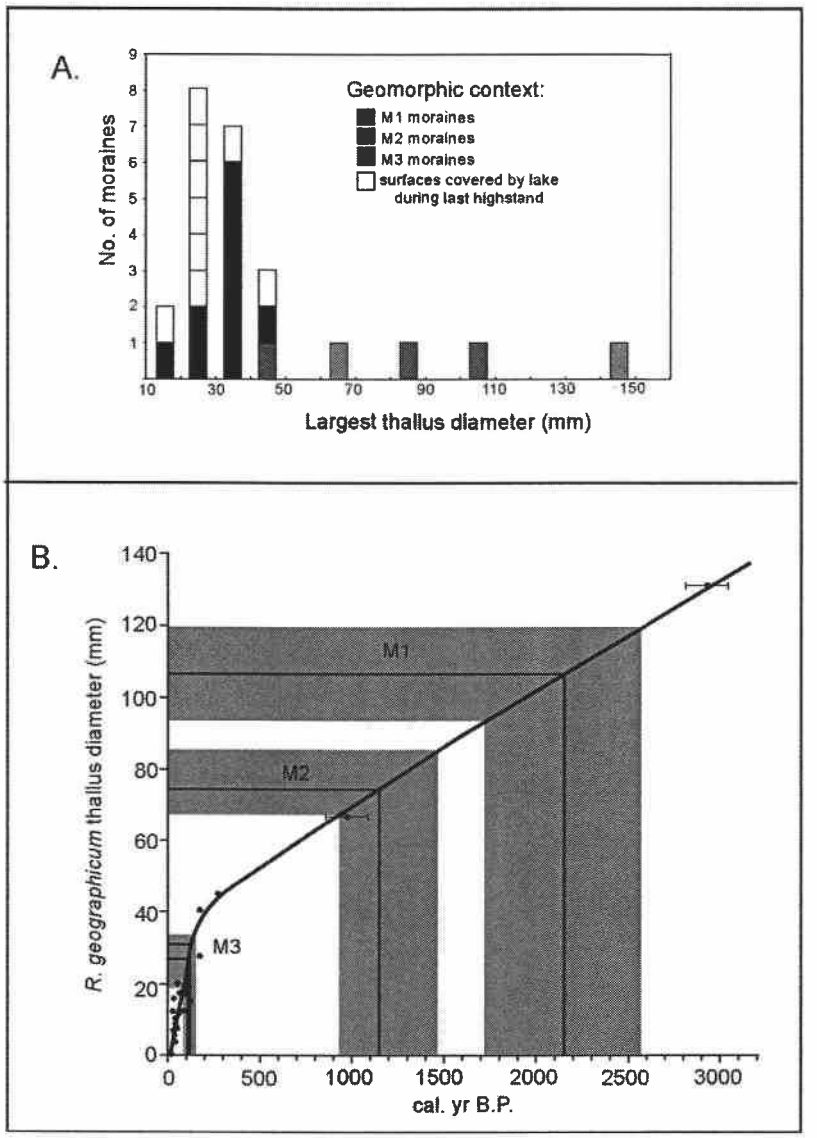

Figure 11. Results of lichenometry. (A) Largest lichen diameters for surfaces according to their geomorphic context binned into 10-mm increments. (B) Lichen diameters plotted on a growth curve developed for the White River (Denton and Karlen, 1977) and used in the Wrangell Mountains (Wiles et al., 2002). Dots are individual control points from tree-rings, radiocarbon ages, or thalli on historic landmarks. M1, M2, and M3 moraines have distinct lichenometric ages (± 20% error estimate in gray). Their ages coincide with periods of moraine-stabilization identified in the White River region (Fig. 4) including two Neoglacial advances separated by ~1000 yrs (M1 and M2), and a LIA advance (M3).

Two radiocarbon ages indicate the presence of older material below 605 m elevation in section 1 (Fig. 9). A sample of fine-grained sediment containing woody debris, collected at 602 m elevation, gave a radiocarbon age of 870 ± 130 cal yrs B.P. A grassy horizon at 604 m elevation yielded an age of 880 ± 100 cal yrs B.P. Sample 3, a piece of wood less than 0.5 m above this grassy horizon, yielded an age of 430 ± 90 cal yrs B.P., which is consistent with deposition during the LIA. The two samples are separated by an oxidation horizon containing organic material ~0.1 m thick, interpreted to represent a period of nondeposition, subaerial exposure, and incipient soil development (Fig. 9). The concordant ages from the lower part of the section indicate that the lower part of section 1 was deposited 800-1000 yrs B.P., and was followed by a depositional hiatus that lasted until the onset of LIA deposition in the basin.

Discussion

Sequence of events in the basin

Sediment delivery out of Granite Creek catchment into the Tana-Chitina River system is modulated by the thickness of Tana Glacier. During periods of Tana Glacier advance, Granite Creek is dammed, a lake forms, and sediment produced in the catchment is stored as fluvial and lacustrine deposits (Fig. 8). Lichenometric ages of moraines suggest that retreat of alpine glaciers within the basin from their LIA termini was well under way by ~100 B.P. Shorelines developed on these moraines indicate the presence of water in the valley during or after the stabilization of the moraines. The highest shorelines occur at an elevation of 710 m, ~100 m above the T1 surface, and

Table 3. Results of radiocarbon analysis

Sample	Material	AA	Lab. No.	d13C	^{14}C age B.P. (1σ)	calibrated (2σ) age range (cal yrs AD)	cal yrs B.P.
1	wood	AA58175	T20070	-26.07	911 ± 64	1000 - 1263 AD	870 ± 130
2	grass	AA58177	T20072	-26.81	914 ± 35	1023 - 1216 AD	880 ± 100
3	grass	AA58176	T20071A	-26.65	294 ± 34	1487 - 1660 AD	430 ± 90
4	grass	AA58180	T20075	-26.63	172 ± 34	1656 - 1950 AD	200 ± 150
5	wood	AA58181	T20076	-25.97	273 ± 53	1479 - 1946 AD	290 ± 230
6	wood	AA58182	T20077R	-26.2	169 ± 34	1657 - 1950 AD	200 ± 150
7	wood	AA58183	T20078	-28.76	141 ± 34	1670 - 1950 AD	190 ± 140

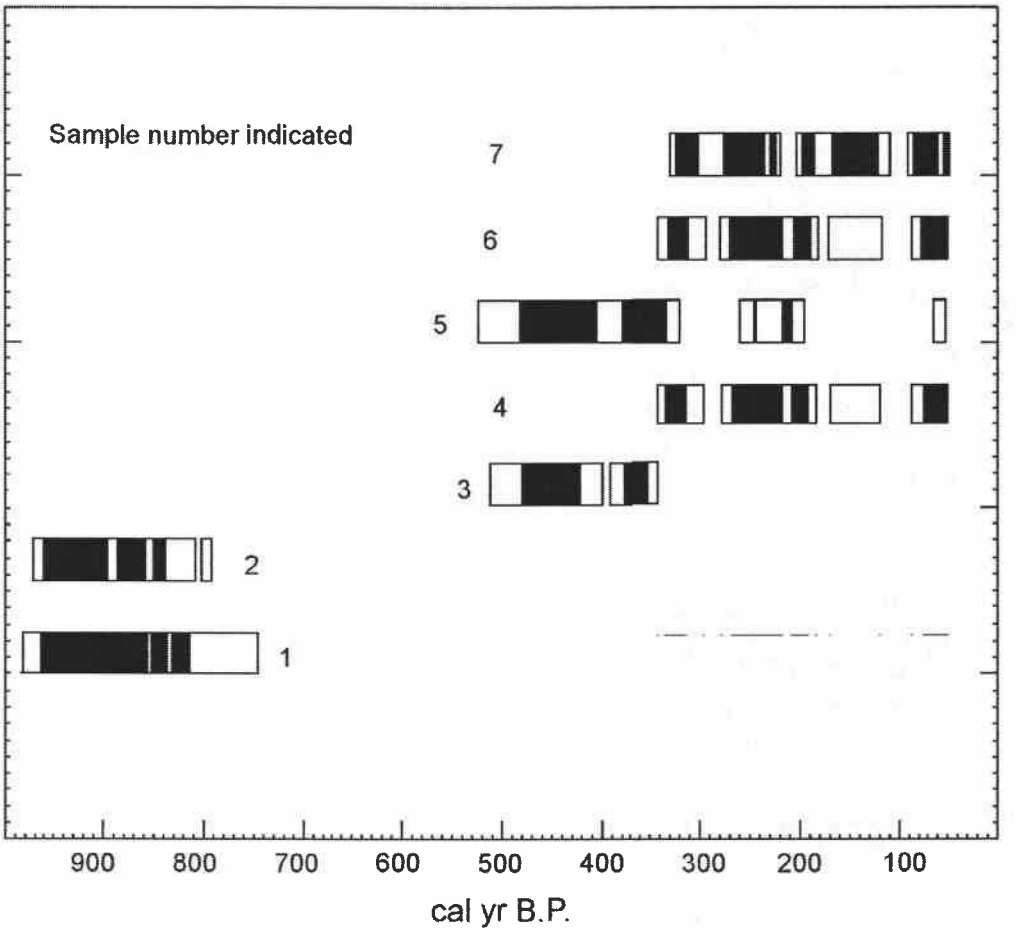

Figure 12. Calibrated age ranges for radiocarbon samples. 1-σ range is highlighted in black, while the white boxes indicate the reported 2-σ age range.

~60 m above either of the Tana Glacier lateral moraines developed across the outlet of the valley. Based on the elevation of the maximum lake level shoreline, the basin contained ~ 5.9 km^3 water, had a surface area of ~ 50 km^2, and extended >10 km up-valley at its maximum.

A gradual shift in facies up the basin from lacustrine sediment to proximal glaciolacustrine deltaic facies reflects backfilling of the basin during lake level rise (Fig. 9). Meltwater from the unnamed glacier to the east of the basin and Twelvemile Creek represent the primary source for input to the lake; other sources included tributary streams originating from alpine glaciers along Thompson Ridge and a meltwater channel sourced from Tana Glacier. These sources likely fluctuated seasonally, which may have resulted in greater sediment delivery during the summer relative to that in the winter. Occasional bands of coarse debris within the laminated muds, along with the debris-covered surface characteristic of the T1 surface, suggest periodic sediment delivery from iceberg-rafted sources, which, based on the elevation of the shorelines, would have originated from the Tana Glacier ice or from glaciers 1-4.

According to the relative elevations of the highest shoreline (710 m) and Tana Glacier's lateral moraines (650 m) and LIA trimlines (730 m), damming of Granite Creek was not controlled by the formation of a moraine dam, but by the height of ice in the Tana Valley (Fig. 8). The level of reservoir height in ice-dammed lakes is often controlled by subglacial drainage (Johnson, 1997; Roberts et al., 2003). Thus, a combination of post-LIA thinning of the Tana Glacier, the configuration of the subglacial drainage network, and incision through valley fill at the outlet of Granite Creek valley modulated the lake level and subsequent drainage of the lake.

Several lake drainage scenarios can be postulated. Rapid drainage from the lake due to outburst would result in catastrophic drainage of water, and rapid knickpoint migration upstream and incision into the unconsolidated muds. Alternatively, slow drainage of the lake controlled by gradually thinning ice would be characterized by progradation of deltaic facies downstream, and punctuated incision and lateral migration of the fluvial system. The lowering rate likely responded to seasonal changes marked by relatively rapid drainage during summer months due to an active subglacial drainage network, which subsequently shuts down during winter.

All geomorphic evidence in the valley supports a slower, possibly seasonal, drainage of the lake during the glacier thinning and retreat following the LIA. A series of about 30 gravelly shorelines ~1-2 vertical meters apart on a glacier 2 moraine indicates periods of relative stability during lake draw-down, supporting slow or periodic drainage. Preservation of the five paired terraces is consistent with alternating incision and lateral migration of the fluvial network into the valley fill. Five terrace levels were identified, indicating >1 km of lateral migration of the fluvial system. At T2 time, for example, the base level of Granite Creek was relatively stable, and allowed for 1.2 km of lateral channel migration.

The geomorphology, sedimentology, and chronology of events within Granite Creek document a cycle of filling and emptying over the LIA glacial cycle. Filling of the lake likely began as thickening of Tana Glacier ice accompanied regional LIA cooling, which may have begun as early as 800-700 cal yrs B.P. (Denton, 1974). Lake level highstand occurred at the same time as or subsequent to stabilization of M3 glacial

moraines. Lake drainage out of Granite Creek valley occurred since the end of the LIA in no more than ~100 yrs.

The presence of ~800-1000 yr B.P. lacustrine sediment beneath the T1 surface in the southwest corner of the valley (Figs. 5 and 9) indicates several things about the nature of valley filling, storage of sediment, and incision of Granite Creek. These deposits are evidence that sediment was deposited in a lacustrine environment at some earlier time within Granite Creek and have been stored since that time, as Granite Creek has not completely evacuated the valley fill from the basin. The present configuration of fluvial terraces, along with the evidence for older deposits in the southwest corner of the valley behind Tana's lateral moraines (Fig. 5), suggest that this site is essentially protected from incision of Granite Creek. A refuge from erosion is consistent with the fact that the Granite Creek outlet is localized along the northern side of the valley. Whereas 900 yr B.P.-deposits below ~605 m elevation represent an earlier climatically-controlled cycle of lake formation due to damming by Tana Glacier, whether the deposits are related to M2, M3, or another advance can not be determined.

Volumes of sediment transfer

The volume of sediment evacuated from the basin following lake drainage was estimated by subtracting the present valley surface from a horizontal surface representing the bottom of the lake (T1 surface; Fig.13; appendix B contains the output from gridding software for these calculations). The calculation reveals that 1.3×10^8 m^3 sediment has been removed from the lake basin by Granite Creek since the end of the LIA. If the LIA ended in AD 1900, this represents an average removal rate of 1.3×10^6 m^3 yr^{-1}, although

the evacuation rate from the basin was probably non-linear and may resemble the exponential decay exhaustion model for paraglacial response proposed by Ballantyne (2002a).

A minimum estimate of the volume of sediment being stored over multiple glacial cycles behind the Tana lateral moraines in Granite Creek can be estimated as well. The 2 radiocarbon ages from the lower part of section 1 indicate deposition of that material behind these moraines below ~600 m elevation was deposited at least 800-1000 yrs B.P.. Paired with the observation that Granite Creek is presently incising through lacustrine deposits 30 m below this unconformity, these ages indicate that at least 4.0×10^7 m^3 sediment has been stored since at least ~1000 yrs B.P.. Because valley fill is still being incised by Granite Creek at the outlet, this number is likely a significant underestimate of the volume of material that is currently stored as valley fill in Granite Creek valley. Based on the sedimentology below the unconformity, much of this material was likely deposited in a lacustrine environment. The presence of this volume of material reflects the fact that material is incompletely evacuated on a single cycle and that storage of material in Granite Creek occurs over multiple Holocene glacial cycles (10^3-10^4 yrs).

Response of unglaciated tributary catchments to deglaciation

Sediment release from Granite Creek is modulated by the thickness of Tana Glacier ice. As ice thickened in the Tana valley, Granite Creek was impounded, lake level rose and sediment produced in the catchment was trapped in the reservoir. This filling may have taken place over the span of the LIA, indicating at least a 300-yr

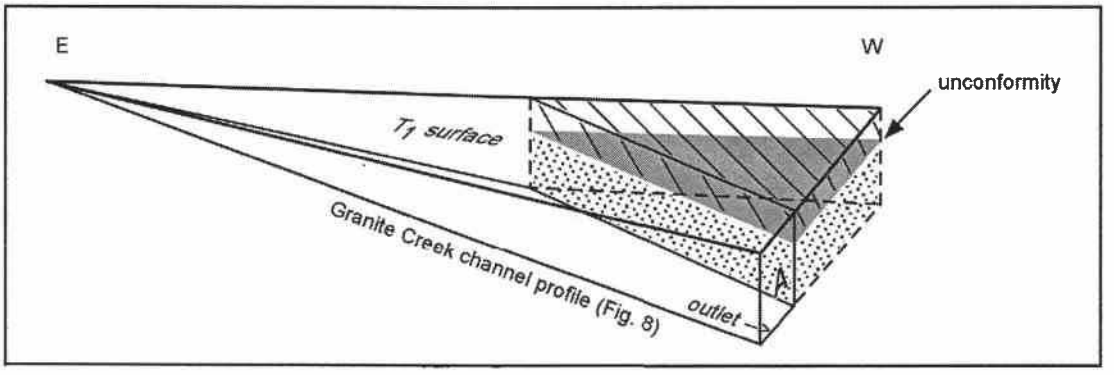

Figure 13. Schematic drawing of Granite Creek valley illustrating sedimentary packages used for volume calculations. Grids representing the surfaces outlined above were created in gridding software based on GPS data collected in the field and DEM analysis. Solid lines represent areas where GPS or DEM data constrain the geometry of the valley. Dashed lines are conceptual geometries used for calculations. The volume of wedge A represents the amount of material that has been evacuated from the basin since removal of the ice dam.

timescale. By contrast, release of sediment since the end of the LIA has taken place rather quickly; lake drainage and vertical incision into at least 40 m of lacustrine sediment has taken place in no more than 100 yrs. The timescale of lake filling and emptying in Granite Creek indicates an out-of-phase relationship between sediment production in and sediment removal from Granite Creek valley on 10^2-10^3 timescales.

This relationship between the timing of sediment production and that of sediment delivery is emblematic of the paraglacial cycle (Fig. 1). Paraglacial sediment release from the landscape may provide a solution to the disconnect between low erosion rates for southern Alaska calculated from low-temperature thermochronometry and the relatively high rates derived from sediment yields (Spotila et al., 2004, Sheaf et al., 2003, Jaeger et al., 1998, Hallet et al., 1996).

In the case of Granite Creek, deglaciation profoundly impacts the release of sediment from the landscape. The paraglacial concept describes deglaciation as characterized by the exposure of unstable and metastable deposits to earth-surface processes. In Granite Creek valley, deglaciation is the physical mechanism for sediment release. Thinning and retraction of Tana Glacier is equivalent to dam lowering and reservoir release. It follows that, for Granite Creek valley, a 500 km^2 catchment that contained a 59 km^2 lake at its maximum, changes in climate directly regulate the storage and release of sediment to the Tana and Chitina Rivers downstream.

Climate changes, however, occur at various timescales and with various amplitudes. It is clear that sediment storage and release occur by this means on millennial timescales during the Holocene. It is plausible that this style of sediment transfer can operate on longer timescales and at larger spatial scales. The Copper River

Basin, a regional glaciolacustrine basin in southern Alaska of which the Chitina River is a tributary (Fig. 3), experienced multiple episodes of damming throughout the Pleistocene. Glacial Lake Atna, a large proglacial lake that formed at least during the last glacial maximum within this basin covered between 5200 km^2 and 9000 km^2 (Ferrians, 1989). Glaciolacustrine sediments associated with the former lake are exposed on land in deeply incised channels of the Copper River and its system of tributaries and are a major source of material to the Copper River Delta (Bennett et al., 2002).

Conclusions

Evidence for three episodes of glacial advance is apparent from the geomorphology and lichenometric ages of moraines in the Granite Creek valley. Two Neoglacial advances correspond well with evidence for glacial expansion in nearby White River Valley and the Wrangell Mountains. Little Ice Age moraines in Granite Creek appear to have stabilized by ~ 100 yrs B.P.

The advance of Tana Glacier during the LIA caused damming of Granite Creek and formation of a 50 km^2 ice-dammed lake in the lower 10 km of the valley. Evidence for the lake includes >30 m of lacustrine deposits in the lower valley and shorelines comprising sorted gravel benches associated with alpine glacial moraines in the valley.

The sedimentary stratigraphy within Granite Creek valley records upstream migration of a fluvial/lake interface, deposition of glaciolacustrine deltaic deposits, followed by deposition in a lacustrine environment. Glaciofluvial deltaic deposits overlying rhythmites in section 8 demonstrate likely downstream migration of the river/lake interface during drainage of the lake.

Five fill-cut terrace levels in the valley record lateral migration of Granite Creek during reestablishment of the fluvial system. These terraces comprise gravel-capped sequences of lacustrine sediments and record over 1.2 km of lateral migration of the channel during incision into the valley fill.

Lake filling and emptying in Granite Creek valley is linked to glacier fluctuations during the Holocene. Shorelines in the valley formed during or after stabilization of LIA moraines. Radiocarbon ages from within the valley fill indicate deposition of lacustrine deposits between the mid-1600's and 1900 AD. Lacustrine deposits older than ~900 yrs B.P. are also found in the valley fill, and may record multiple episodes of filling/emptying over Holocene glacial cycles.

Storage and release out of Granite Creek valley is thus modulated by climatic changes over $10^3 - 10^4$ timescales. During the LIA, sediment produced in the Granite Creek catchment over the >300 yr advance and maximum phase was deposited and stored in the lower part of the valley. Glacial retraction since the end of the LIA has caused release of 1.3×10^8 m^3 sediment in no more than ~100 years. This disparity in timescales for storage and release implies that sediment production and sediment delivery to adjacent fluvial networks is out of phase on Holocene glacial timescales. This type of sediment transfer following deglaciation likely contributes significantly to increased sediment yields from catchments following deglaciation.

References

Ager, T.A., 1983. Holocene vegetational history of Alaska. In: Wright Jr., H.E. (Ed.), Late Quaternary Environments of the United States, The Holocene, Vol. 2. University of Minnesota Press, Minneapolis, pp. 128-141.

Alaska Climate Research Center. Alaska Climatology database. Obtained online at http://climate.gi.alaska.edu/Climate/index.html, 14 October, 2004.

Arsenault, M., and Meigs, A., in press. Contribution of deep-seated landslides to erosion of a glaciated basin in southern Alaska. Earth Surface Processes and Landforms.

Ashmore, P., 1993. Contemporary erosion of the Canadian landscape. Progress in Physical Geography 17, 190-204.

Ballantyne, C.K., 2002a. A general model of paraglacial landscape response. The Holocene 12, 371-376.

Ballantyne, C.K., 2002b. Paraglacial Geomorphology. Quaternary Science Reviews 21, 1935-2017.

Bennett, M.R., Huddart, D., and Thomas, G.S.P., 2002. Facies architecture within a regional glaciolacustrine basin: Copper River, Alaska. Quaternary Science Reviews 21, 2237-2279.

Boothroyd, J.C., and Ashley, G.M., 1975. Processes, bar morphology, and sedimentary structures on braided outwash fans, northeastern Gulf of Alaska. In: Jopling, A.V., and McDonald, B.C. (Eds.), Glaciofluvial and glaciolacustrine sedimentation, Special Publication-Society of Economic Paleontologists and Mineralogists, Iss. 23, pp. 193-222.

Calkin, P.E., Wiles, G.C., and Barclay, D.J., 2001. Holocene coastal glaciation of Alaska. Quaternary Science Reviews 20, 449-461.

Church, M., and Ryder, J.M., 1972. Paraglacial sedimentation: A consideration of fluvial processes conditioned by glaciation. Geological Society of America Bulletin 83, 3059-3072.

Church, M., and Slaymaker, O., 1989. Disequilibrium of Holocene sediment yield in glaciated British Columbia. Nature 337, 452-454.

Denton, G.H., 1974. Quaternary glaciations of the White River Valley, Alaska, with a regional synthesis for the northern St. Elias Mountains, Alaska, and Yukon Territory. Geological Society of America Bulletin 85, 871-892.

Denton, G.H., and Karlen, W., 1977. Holocene glacial and tree-line variations in the White River Valley and Skolai Pass, Alaska and Yukon Territory. Quaternary Research 7, 63-111.

Evenson, E.B., and Clinch, J. M., 1987. Debris transport mechanisms and active alpine glacier margins: Alaskan case studies. Geological Survey of Finland, Special Paper 3, 111-136.

Eyles, N., and Miall, A.D., 1984. Glacial facies. In: Walker, R.G. (Ed.), Geoscience Canada Reprint Series 1, pp. 15-38.

Eyles, N., Eyles, C.H., and Miall, A.D., 1983. Lithofacies types and vertical profile models; an alternative approach to the description and environmental interpretation of glacial diamict and diamictite sequences. Sedimentology 30, 393-410.

Ferrians Jr., O.J., 1989. Glacial Lake Atna, Copper River Basin, Alaska. In: Carter, L.D., Hamilton, T.D., Galloway, J.P. (Eds.), Late Cenozoic History of the Interior Basins of Alaska and the Yukon, United States Geological Survey, Circular 1026, pp.85-88.

Gustavson, T.C., Ashley, G.M., and Boothroyd, J.C., 1975. Depositional sequences in glaciolacustrine deltas. In: Jopling, A.V., and McDonald, B.C. (Eds.) Glaciofluvial and Glaciolacustrine Sedimentation. Society of Economic Paleontologists and Mineralogists, Tulsa, pp. 264-280.

Hallet, B., Hunter, L., and Bogen, J., 1996. Rates of erosion and sediment evacuation by glaciers: A review of field data and their implications. Global and Planetary Change 12, 213-235.

Hamilton, T.D., 1994. Late Cenozoic glaciation of Alaska. In: Plafker, G., Berg, H.C. (Eds.), The geology of Alaska. Geological Society of America, Boulder, pp. 813-844.

Harbor, J., and Warburton, J., 1993. Relative rates of glacial and nonglacial erosion in alpine environments. Arctic and Alpine Research 25, 1-7.

Heusser, C.J., 1995. Late-Quaternary vegetation response to climatic-glacial forcing in North Pacific America. Physical Geography 16, 118-149.

Hinderer, M., 2001. Late Quaternary denudation of the Alps, valley and lake fillings and modern river loads. Geodinamica Acta 14, 231-263.

Hodgkins, R., Cooper, R., Wadham, J., and Tranter, M., 2003. Suspended sediment fluxes in a high-Arctic glacierised catchment: implications for fluvial sediment storage. Sedimentary Geology 162, 105-117.

Hudson, T. and Plafker, G., 1982. Paleogene metamorphism of an accretionary flysch terrane, eastern Gulf of Alaska. Geological Society of America Bulletin 93, 1280-1990.

Humphrey, N.F., and Raymond, C.F., 1994. Hydrology, erosion and sediment production in a surging glacier; Variegated Glacier, Alaska, 1982-1983.

Jaeger, J.M., Nittrouer, C.A., Scott, N.D., and Milliman, J.D., 1998. Sediment accumulation along a glacially impacted mountainous coastline: Northeast Gulf of Alaska. Basin Research 10, 155-173.

Johnson, P.G., 1997. Spatial and temporal variability of ice-dammed lake sediments in alpine environments. Quaternary Science Reviews 16, 635-647.

Johnston, S., Meigs, A., Garver, J., and Spotila, J., 2004. Backstop and orogenic wedge cooling history in the active Yakutat Terrane collision, southern Alaska. Geological Society of America Abstracts with Programs 36-5, p. 270.

Koppes, M. N., and Hallet, B., 2002. Influence of rapid glacial retreat on the rate of erosion by tidewater glaciers. Geology 30, 47-50.

Lagoe, M.B., Eyles, C.H., Eyles, N., and Hale, C., 1993. Timing of Late Cenozoic tidewater glaciation in the far North Pacific. Geological Society of America Bulletin 105, 1542-1560.

Lamoureux, S.F., 1999. Catchment and lake controls over the formation of varves in monomictic Nicolay Lake, Cornwall Island, Nunavut. Canadian Journal of Earth Sciences 36, 1533-1546.

Luckman, B.H., 2000. Little Ice Age in the Canadian Rockies. Geomorphology 32, 357-384.

Meigs, A., and Sauber, J., 2000. Southern Alaska as an example of the long-term consequences of mountain building under the influence of glaciers. Quaternary Science Reviews 19, 1543-1562.

Miall, A.D., 1978. Lithofacies types and vertical profile models in braided river deposits: a summary. In: Miall, A.D. (Ed.), Fluvial Sedimentology. Canadian Society of Petroleum Geologists Memoir 5, 597-604.

Molnar, P., and England, P., 1990. Late Cenozoic uplift of mountain ranges and global climatic changes: chicken or egg? Nature 346, 29-34.

O'Sullivan, P.B., and Currie, L.D., 1996. Thermotectonic history of Mt. Logan, Yukon Territory, Canada. Earth and Planetary Science Letters 144, 251-261.

Pewe, T.L., 1975. Quaternary geology of Alaska. United States Geological Survey Professional Paper, 145 pp.

Phillips, J.D., 1991. Fluvial sediment budgets in the North Caroline Piedmont. Geomorphology 4, 231-241.

Plafker, G., and Addicott, W.O., 1976. Glaciomarine deposits of Miocene through Holocene age in the Yakataga Formation along the Gulf of Alaska margin, Alaska. United States Geological Survey Open File Report, Reston, pp. 45.

Plafker, T.L., 1987. Regional geology and petroleum potential of the northern Gulf of Alaska continental margin. In: Scholl, D.W., Grantz, A., Vedder, J.G. (Eds.), Geology and Petroleum Potential of the Continental Margin of Western North America and Adjacent Ocean Basins-Beaufort Sea to Baja California. Texas, circum-pacific council for energy and mineral resources. Earth Science Series, Houston, TX, pp. 229-268.

Porter, S.C., 1989. Late Holocene fluctuations of the fjord glacier system in Icy Bay, Alaska. Arctic and Alpine Research 21 (4), 364-379.

Post, A., and Mayo, L.R., 1971. Glacier dammed lakes and outburst floods in Alaska. United States Geological Survey Hydrologic Investigations Atlas HA-455, 10 pp.

Roberts, M.J., Tweed, F.S., Russel, A.J., Knudsen, O., and Harris, T.D., 2003. Hydrologic and geomorphic effects of temporary ice-dammed lake formation during jokulhlaups. Earth Surface Processes and Landforms 28, 723-737.

Shaw, J., 1977. Sedimentation in an alpine lake during deglaciation, Okanagan Valley, British Columbia, Canada. Geografiska Annaler, Series A, Physical Geography 59, 221-240.

Sheaf, M.A., Serpa, L., and Pavlis, T.L., 2003. Exhumation rates in the St. Elias Mountains, Alaska. Tectonophysics 367, 1-11.

Solomina, O. and Calkin, P., 2003. Lichenometry as applied to moraines in Alaska, U.S.A., and Kamchatka, Russia. Arctic, Antarctic and Alpine Research 35, 129-143.

Spotila, J.A., Buscher, J.T., Meigs, A.J., and Reiners, P.W., 2004. Long-term glacial erosion of active mountain belts; example of the Chugach-St. Elias Range, Alaska. Geology 32, 501-504.

Suess, H.E., 1980. The radiocarbon record in tree rings of the last 8,000 years. Radiocarbon 22, 200-209.

Warburton, J., 1999. Environmental change and sediment yield from glacierised basins: the role of fluvial processes and sediment storage. In: Brown, A.G., and Quine, T.A. (Eds.), Fluvial Processes and Environmental Change. John Wiley and Sons, Ltd., Chichester, pp. 363-384.

Wiles, G.C., Jacoby, G.C., Davi, N.K., and McAllistor, R.P., 2002. Late Holocene glacier fluctuations in the Wrangell Mountains, Alaska. Geological Society of America Bulletin 114, 896-908.

Yager, E.M., Barclay, D.J., Calkin, P.E., and Wiles, G.C., 1998. Tree-ring based history of Sheridan Glacier, southern Alaska. Geological Society of America Abstracts with Programs 30, 80.

APPENDICES

Appendix A. Lichenometric data.

The measurements (in mm) of individual lichen thalli from Granite Creek Valley surfaces can be found in the table below.

Table 4. Individual lichen thalli measurements.

L1	41,41,31,30,30,27,27,27,26,26,25,24,24,24,23,23,23,23,23,23,23,22,22,22,21,21,21,20,20,20,20,19,19,19,18,18,18,18,18,17,17,17,16,16,15,14
L2a	34,34,34,33,32,32,30,30,30,30,30,29,29,28,28,27,27,27,27,26,26,26,26,26,25,25,25,25,25,24,24,24,24,24,24,23,23,23,22,20,20,20,20,20,19,19,19,18,18,18,18,18,16,15,8
L2b	50,47,38,34,33,32,30,30,30,29,28,27,27,27,27,27,26,26,25,25,24,23,22,21,21,19,19,19,18,18,16,16,15
L3	38,27,27,26,24,22,21,21,20,20,20,20,19,19,19,18,18,17,17,16,14
L4	34,31,29,26,26,26,25,25,24,23,23,23,23,22,22,22,21,21,21,21,21,20,20,20,20,20,20,18,18,18,17,17,17,17,16,13
L5	40,33,32,31,30,30,29,28,28,27,26,26,25,25,25,25,25,25,25,25,25,24,24,23,23,22,22,21,19
L6	31,30,30,30,27,27,26,25,24,24,24,23,23,23,23,22,22,22,21,21,21,21,21,20,20,20,19,18,18,17,17,16,15,15
L7	47,46,46,43,43,42,42,41,41,39,39,39,38,38,38,38,38,37,37,37,37,36,36,36,35,35,35,34,34,34,34,34,33,32,32,32,32,32,32,31,31,31,28,28,26
L8	38,37,37,37,37,36,36,36,35,33,32,31,31,31,31,31,31,31,30,30,30,30,30,30,29,29,29,28,28,28,28,28,27,27,27,27,25,25,25,25,25,24,24,24,21,20
L9	114,100,75,64,64,61,59,58,58,54,47,45,43,38,37
L10	27,25,23,21,21,21,21,20,20,20,18,17,17,17,17,17,16,16,16,16,16,16,16,15,15,15,15,14,14,14,13,13,13,11,10,10,9,9,6,4
L11	34,34,34,33,33,33,32,31,27,26,26,26,25,25,25,24,24,24,24,23,23,23,23,22,22,22,21,20,19,19,18,18,18,16
L12	25,24,23,23,23,22,22,22,22,21,21,21,21,21,20,20,20,20,20,19,19,19,19,19,18,18,18,18,18,18,17,17,16,16,16,16,16,15
L13	21,17,17,16,16,15,14,14,13,13,12,12,11,11,10,9,8
L14	26.2,24.8,22.8,21.1,21,19.2,19.1,19.1,19,19,17.8,17.3,17,16.5,16.2,16,15.3,15,15,14.9,13.2
L15	45.5,38,37.8,34.8,34.4,33,32.3,32,31.2,28.8,28,27.9,27.2,26.2,26,24.2,21
L16	94,65.4,64.3,61.9,55,52,45.5,28.1
L17	19.8,16.4,16.3,16.1,16,15.8,15.5,12.8,12,11.8,11.2,11,10.8
a	23,22,22,19,16,15,15,15,14,14,14
b	29,27,22,19,18,17,16,14
c	41,32,32,29,27,26,25,24,22,22,22,21,21,21,21,21,21,20,20,19,19,19,19,18,18,17,16,16,13
e	35,33,33,30,30,29,28,28,28,28,27,25,25,25,22
f	120,114,110,92,90,89,89,89,88,87,87,86,85,84,83,82,82,82,82,82,80,80,75
g	150,150,140,135,133,128,117,115,110,107,105,100,99,95,93,89,89,80,80,78,75

Appendix B. Volume calculations.

The results of the volumetric estimates derived using Golden Software's Surfer gridding software are found below. Two volumetric estimates, one for the volume of material removed from lower Granite Creek since the removal of the ice dam, and one for the volume of the lake during the maximum lake level, were performed using grid data compiled from a USGS 30-m DEM and from GPS data collected in the field. The volume of material evacuated from the basin (table 5) was derived by subtracting the present surveyed land surface in the valley from the 620-m elevation of the T1 surface, the surface interpreted to represent the bottom of the lake. This volume is roughly 1.3×10^8 m^3. The volume of the lake (table 6) was estimated by subtracting the USGS 30-m DEM of Granite Creek Valley from the 710-m elevation of the highest shoreline, interpreted to be the highstand of the lake, giving a volume of 6.0×10^9 m^3. This volume includes some amount of the previously calculated volume of evacuated material, depending on when the USGS topographic maps were created; however, the volume of the volume of evacuated material is an order of magnitude smaller than that of the lake, and does not change the estimate of the total lake volume significantly.

Table 5. Estimate of volume of material evacuated from the basin:	
Upper Surface	
Level Surface defined by Z = 619.9	
Lower Surface	
Grid Size:	50 rows x 200 columns
X Minimum:	410841.3721
X Maximum:	418740.7648
X Spacing:	39.6954407
Y Minimum:	6733383.549
Y Maximum:	6735291.367
Y Spacing:	38.935061
Z Minimum:	568.324
Z Maximum:	620
Volumes	
Z Scale Factor:	1
Total Volumes by:	
Trapezoid Rule:	126318743.68409
Simpson's Rule:	125929302.72616
Simpson's 3/8 Rule:	126208263.14635
Cut & Fill Volumes:	
Positive Volume (Cut):	127179270.33743
Negative Volume (Fill):	860591.051022
Net Volume (Cut-Fill):	126318679.28641

Table 6. Estimate of lake volume:	
Dataset:	USGS 30-m DEM
Type:	Raster
ZFactor:	1
Plane_Height:	710.00
Reference:	Below_Plane
Volume:	6013472870.82